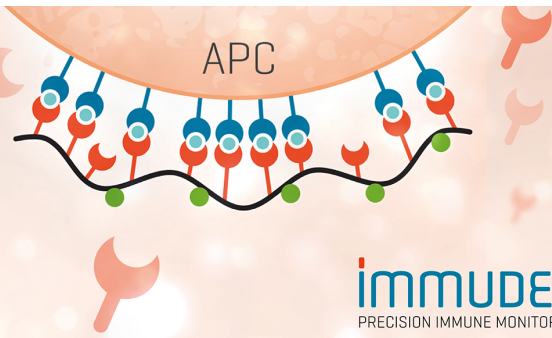


## TCR Solutions Detect Antigen Presentation

- Immunex produces your TCRs
- Soluble TCRs and TCR Dextramer®



**IMMUDEx**<sup>®</sup>  
PRECISION IMMUNE MONITORING

## The Journal of Immunology

RESEARCH ARTICLE | JUNE 01 2010

### V $\gamma$ 2V $\delta$ 2 T Cell Receptor Recognition of Prenyl Pyrophosphates Is Dependent on All CDRs

Hong Wang; ... et. al

*J Immunol* (2010) 184 (11): 6209–6222.

<https://doi.org/10.4049/jimmunol.1000231>

#### Related Content

Sensor Function for Butyrophilin 3A1 in Prenyl Pyrophosphate Stimulation of Human V $\gamma$ 2V $\delta$ 2 T Cells

*J Immunol* (November,2015)

Structural Features of Nonpeptide Prenyl Pyrophosphates That Determine Their Antigenicity for Human  $\gamma\delta$  T Cells

*J Immunol* (July,2001)

Butyrophilin 3A1 Plays an Essential Role in Prenyl Pyrophosphate Stimulation of Human V $\gamma$ 2V $\delta$ 2 T Cells

*J Immunol* (August,2013)

# V $\gamma$ 2V $\delta$ 2 T Cell Receptor Recognition of Prenyl Pyrophosphates Is Dependent on All CDRs

Hong Wang, Zhimei Fang, and Craig T. Morita

$\gamma\delta$  T cells differ from  $\alpha\beta$  T cells in the Ags they recognize and their functions in immunity. Although most  $\alpha\beta$  TCRs recognize peptides presented by MHC class I or II, human  $\gamma\delta$  T cells expressing V $\gamma$ 2V $\delta$ 2 TCRs recognize nonpeptide prenyl pyrophosphates. To define the molecular basis for this recognition, the effect of mutations in the TCR CDR was assessed. Mutations in all CDR loops altered recognition and cover a large footprint. Unlike murine  $\gamma\delta$  TCR recognition of the MHC class Ib T22 protein, there was no CDR3 $\delta$  motif required for recognition because only one residue is required. Instead, the length and sequence of CDR3 $\gamma$  was key. Although a prenyl pyrophosphate-binding site was defined by Lys109 in J $\gamma$ 1.2 and Arg51 in CDR2 $\delta$ , the area outlined by critical mutations is much larger. These results show that prenyl pyrophosphate recognition is primarily by germline-encoded regions of the  $\gamma\delta$  TCR, allowing a high proportion of V $\gamma$ 2V $\delta$ 2 TCRs to respond. This underscores its parallels to innate immune receptors. Our results also provide strong evidence for the existence of an Ag-presenting molecule for prenyl pyrophosphates. *The Journal of Immunology*, 2010, 184: 6209–6222.

**T** cells can be divided into two distinct subsets,  $\gamma\delta$  and  $\alpha\beta$ , based on their expression of rearranging adaptive TCRs.  $\gamma\delta$  T cells, mucosal-associated invariant  $\alpha\beta$  T cells (1), and invariant NK  $\alpha\beta$  T cells (iNKTs) (2, 3) are innate lymphocytes that bridge innate and adaptive immunity through their recognition of unconventional ligands. The major subset of human  $\gamma\delta$  T cells expresses V $\gamma$ 2V $\delta$ 2 TCR (also termed V $\gamma$ 9V $\delta$ 2 or TRGV9TRDV2). Although a minor subset at birth (4), V $\gamma$ 2V $\delta$ 2 T cells expand between the ages of 1–10 y old (5). This expansion is not due to genetic causes because identical twins can differ in their proportions of V $\gamma$ 2V $\delta$ 2 T cells. Instead, a broad array of bacterial and protozoal infections expand V $\gamma$ 2V $\delta$ 2 T cells to large numbers (>50% of blood T cells in some cases) (reviewed in Ref. 6).

The broad reactivity of V $\gamma$ 2V $\delta$ 2 T cells to microbes and some tumors was explained by the finding that nonpeptide prenyl pyrophosphates, such as isopentenyl pyrophosphate (IPP), act as Ags for V $\gamma$ 2V $\delta$ 2 T cells (7). Prenyl pyrophosphates are essential metabolites required by all organisms. The recognition of microbes by V $\gamma$ 2V $\delta$ 2 T cells is due to the preferential recognition of (*E*)-4-hydroxy-3-methyl-but-2-enyl pyrophosphate (HMBPP) over IPP (HMBPP is 30,000-fold more active than IPP on

a molar basis) (8, 9). HMBPP is a metabolite in the 2-*C*-methyl-D-erythritol-4 phosphate pathway for isoprenoid biosynthesis. This pathway is used by most Eubacteria (including all mycobacteria and Gram-negative rods) and Apicomplexan protozoa (the causative agents of malaria, toxoplasmosis, babesiosis, and cryptosporidiosis). Other stimulating compounds, such as bisphosphonates (10, 11) and alkylamines (12), act by increasing cellular IPP levels by blocking farnesyl pyrophosphate (FPP) synthase in the mevalonate pathway (13, 14).

V $\gamma$ 2V $\delta$ 2 T cells function in both microbial and tumor immunity. The early expansion of V $\gamma$ 2V $\delta$ 2 T cells to prenyl pyrophosphates results in conversion to memory cells (C. Jin and C.T. Morita, unpublished observations) (15) capable of mounting adaptive responses to *Mycobacterium bovis* bacillus Calmette-Guérin (BCG) (16) and other infections. As memory cells, V $\gamma$ 2V $\delta$ 2 T cells can mount rapid responses to primary microbial infections with organisms using the 2-*C*-methyl-D-erythritol-4 phosphate pathway (9). Activation of V $\gamma$ 2V $\delta$ 2 T cells leads them to release Th1 cytokines, including IFN- $\gamma$ , TNF- $\alpha$ , and GM-CSF, but not IL-2 (17, 18), and to secrete chemokines, such as MIP-1 $\alpha$  (CCL3), MIP-1 $\beta$  (CCL4), lymphotactin (XCL1), and RANTES (CCL5) (19, 20). V $\gamma$ 2V $\delta$ 2 T cells are potent killer cells and can lyse infected cells via perforin and/or Fas-Fas ligand pathways (21) and kill released bacteria and protozoa through production of granulysin (21, 22) and the cathelicidin LL-37 (23). Activated V $\gamma$ 2V $\delta$ 2 T cells also kill tumor cells from a variety of tissue origins through both TCR- and NK receptor-mediated recognition (reviewed in Ref. 6). Treatment with bisphosphonates and IL-2 activates V $\gamma$ 2V $\delta$ 2 T cells, leading to stable disease or partial remissions in some patients with B cell malignancies (24) or with metastatic prostate cancer (25). There are presently several ongoing clinical trials examining immunotherapy with V $\gamma$ 2V $\delta$ 2 T cells for a variety of cancers.

Recognition of prenyl pyrophosphates is mediated by the V $\gamma$ 2V $\delta$ 2 TCR because transfection of the V $\gamma$ 2V $\delta$ 2 TCR to  $\beta^-$  Jurkat cells confers reactivity to prenyl pyrophosphates and Daudi and RPMI-8226 tumor cell lines (26). We and others proposed that reactivity to the negatively charged prenyl pyrophosphates was dependent on positively charged residues in a potential prenyl pyrophosphate-binding site located in V $\gamma$ 2V $\delta$ 2 TCR (27, 28). Consistent with this hypothesis, reactivity was dependent on N-encoded amino acid

Division of Rheumatology, Department of Internal Medicine, Interdisciplinary Graduate Program in Immunology, University of Iowa College of Medicine, Iowa City, IA 52242

Received for publication January 25, 2010. Accepted for publication March 31, 2010.

This work was supported by grants from the National Institutes of Health, National Institute of Arthritis and Musculoskeletal and Skin Disease (AR45504), the National Institute of Allergy and Infectious Diseases (Midwest Regional Center of Excellence for Biodefense and Emerging Infectious Diseases Research, AI057160), and the National Cancer Institute (CA113874) to C.T.M.

Address correspondence and reprint requests to Dr. Craig T. Morita, Division of Rheumatology, Department of Internal Medicine, Interdisciplinary Graduate Program in Immunology, University of Iowa College of Medicine, EMRB 400F, Iowa City, IA 52242. E-mail address: craig-morita@uiowa.edu

The online version of this article contains supplemental material.

Abbreviations used in this paper: BSA, buried surface area; HMBPP, (*E*)-4-hydroxy-3-methyl-but-2-enyl pyrophosphate; iNKT, invariant NK  $\alpha\beta$  T cell; IPP, isopentenyl pyrophosphate.

Copyright © 2010 by The American Association of Immunologists, Inc. 0022-1767/10/\$16.00

residues in the junctional segment of the V $\gamma$ 2 chain (29) as well as lysine residues in the J $\gamma$ 1.2 segment (also termed J $\gamma$ P), an arginine residue in CDR2 $\delta$ , and an aliphatic amino acid residue in CDR3 $\delta$  (30, 31).

Despite identification of a potential prenyl pyrophosphate-binding site, there was no evidence for prenyl pyrophosphate binding by the V $\gamma$ 2V $\delta$ 2 TCR (28) or direct functional recognition (32). Instead, recognition of prenyl pyrophosphates required cell-cell contact but neither Ag internalization nor processing (32, 33). This is similar to allergic CD4 and CD8  $\alpha\beta$  T cell recognition of small nonpeptide drugs presented by MHC class I or class II molecules (34). In contrast to drug recognition, prenyl pyrophosphate Ag recognition is independent of classical MHC class I, MHC class II,  $\beta_2$ -microglobulin, MICA/MICB, and CD1 molecules (32). Moreover, photoaffinity analogs of prenyl pyrophosphates could form covalent bonds to a putative presenting molecule distinct from known Ag-presenting molecules (35), and tetramers of macaque V $\gamma$ 2V $\delta$ 2 TCR could bind to the surface of human but not mouse cells only in the presence of HMBPP (36).

The available studies suggest, but do not prove, that a presenting molecule exists for prenyl pyrophosphates. To help clarify this issue, we have studied the effect of alanine mutations in residues in CDR1, CDR2, and CDR3 on prenyl pyrophosphate recognition and analyzed CDR3 sequences of reactive V $\gamma$ 2V $\delta$ 2 T cell clones. We find that residues in all CDRs of the V $\gamma$ 2V $\delta$ 2 TCR can affect recognition, but no CDR3 $\delta$  motif is required for recognition beyond the requirement for an aliphatic residue at position 97. Instead, recognition is critically dependent on the V $\gamma$ 2J $\gamma$ 1.2 chain, which is either invariant or has limited diversity in sequence and length. Given the large footprint of the required residues, which surpasses the predicted prenyl pyrophosphate-binding site, it is likely that a presenting molecule is required for prenyl pyrophosphate Ags.

## Materials and Methods

### Cell lines

The mutant Jurkat cell line, J.RT3-T3.5, was obtained from the American Type Culture Collection (Rockville, MD) and is a TCR  $\beta$ -negative variant of Jurkat that lacks TCR cell surface expression (37). J.RT3-T3.5 and J.RT3-T3.5 transfectants were grown in RPMI 1640 supplemented with 10% FCS, 10 mM HEPES, 10  $\mu$ g/ml gentamycin, 5  $\times$  10<sup>-5</sup> M 2-ME, and L-glutamine (Invitrogen, Carlsbad, CA). RPMI 8226 and Raji cells were obtained from the American Type Culture Collection and maintained in the medium described above. The Va2 human fibroblast cell line was obtained from Dr. Charles Stiles (Dana-Farber Cancer Institute) and maintained in DMEM with the additives listed above. Hygromycin B and G418 were obtained from Invitrogen.

### mAbs and Ags

mAbs reactive with the human V $\gamma$ 2V $\delta$ 2 TCR used in this paper were as follows: control mAb (P3), anti-pan TCR $\gamma\delta$  (anti-TCR $\delta$ 1), anti-V $\gamma$ 2 (Ti $\gamma$ A, 7A5, 360, and 4D7), and anti-V $\delta$ 2 (BB3, 4G6, 389, G1, and TiV $\delta$ 2). The specificity of these mAbs was previously reviewed (38). Prenyl pyrophosphates (IPP, dimethylallyl pyrophosphate, and FPP) and alkylamines were purchased from Sigma-Aldrich (St. Louis, MO). Phosphoantigens including monomethyl-, mono-ethyl-, phenethyl-, and isoamyl-pyrophosphate and the nucleotide-conjugated compound, ethyl-deoxyuridine triphosphate were synthesized as described (7, 38). Bromohydrin pyrophosphate, risedronate, and alendronate were provided by Eric Oldfield (University of Illinois at Urbana-Champaign, Champaign, IL). HMBPP was synthesized as previously described (39). KM20 and KM22 are extracts of *Escherichia coli* strain *lytB* mutants that produce a high level of HMBPP (9, 40).

### cDNA cloning and mutagenesis of human V $\gamma$ 2V $\delta$ 2 TCR

RNA was isolated from the human T cell clone DG.SF13 (Micro RNA isolation kit; Stratagene, La Jolla, CA) followed by cDNA synthesis using SuperScript II reverse transcriptase and random hexamers (SuperScript first-

strand synthesis system for RT-PCR; Life Technologies, Gaithersburg, MD). PCR was done with Platinum Taq High Fidelity DNA polymerase (Life Technologies). PCR primers used to derive full-length V $\gamma$ 2C $\gamma$ -chains were as described previously (21). For the V $\delta$ 2C $\delta$ -chain, the following primers were used to introduce an XhoI restriction site into the 5' region and a BamHI site into the 3' region of the V $\delta$ 2C $\delta$ -chain for cloning: 5'-gggctcgagCAGG-CAGAAGGTGGTTGAGAG-3', V $\delta$ 2 5' untranslated region; and 5'-gggggatccGGAGTGTAGCTTCCTCAT-3', V $\delta$ 2 3' untranslated region. The V $\gamma$ 2J $\gamma$ 1.2C $\gamma$ 1 PCR product was cloned into the pREP7 vector (Invitrogen) using the KpnI-XhoI sites. The V $\delta$ 2C $\delta$  PCR product was cloned into the pREP9 vector (Invitrogen) using the XhoI-BamHI sites. For mutagenesis, TCR- $\gamma$  and TCR- $\delta$ -chain cDNAs mutated by a single amino acid residue were generated using QuikChange Site-Directed Mutagenesis Kit (Stratagene). To confirm the mutations, all V $\gamma$ 2C $\gamma$  and V $\delta$ 2C $\delta$  mutants were fully sequenced. Sequencing was done using an automated sequencer using the pREP forward and reverse primers along with the following reverse primers: C $\gamma$  3' UT, ATGGCCCTCTGTGCCACCG; C $\gamma$  internal, 5'-TGTGTCTG-TTAGTCTTCATGG-3'; C $\delta$  3' UT, GGAGTGTAGCTTCCTCATGC; and C $\delta$  internal, 5'-GACAATAGCAGGATCAAACCT-3'.

### Derivation of V $\gamma$ 2V $\delta$ 2 TCR transfectants

Human V $\gamma$ 2V $\delta$ 2 TCR transfectants were derived by electroporation of the Jurkat mutant J.RT3-T3.5, with unmutated or mutated DG.SF13 TCR  $\gamma$ - and  $\delta$ -chain cDNAs, as described previously (41). Briefly, J.RT3-T3.5 cells were grown at low density (1 to 2  $\times$  10<sup>5</sup> cells/ml) prior to use, centrifuged while in log phase growth, and resuspended at 3.33  $\times$  10<sup>7</sup>/ml in PBS containing 10 mM HEPES. A total of 0.3 ml resuspended cells was aliquoted into each electroporation cuvette; 20  $\mu$ g each plasmid (pREP7-TCR- $\gamma$  and REP9-TCR- $\delta$ ) was added to the cells followed by incubation at room temperature for 10 min. The cells were electroporated (960  $\mu$ F, 250 V) using a Gene Pulser (Bio-Rad, Burlingame, CA) and incubated at room temperature for an additional 10 min. The electroporated cells from each cuvette were washed twice in PBS, resuspended into 30 ml complete media, plated in three 96-well round-bottom plates, and cultured at 37°C. After 48 h, hygromycin B was added to 0.5 mg/ml. Transfectants surviving hygromycin B selection were then cultured in media containing both G418 (1 mg/ml) and hygromycin B (0.5 mg/ml). After 2 to 3 wk of culture, transfectants were screened for IL-2 release in response to anti-TCR $\delta$ 1 stimulation. Transfectants specifically responsive to anti-TCR stimulation were expanded at low density and tested for their response to nonpeptide Ags. Multiple transfectants for each mutant that specifically released IL-2 to anti-TCR stimulation were derived from separate transfections and tested to confirm each result (Supplemental Figs. 1, 2). Because defects in Jurkat TCR signaling caused some TCR-expressing transfectants (despite high levels of TCR expression) to either not release IL-2 or to constitutively produce IL-2, only those mutants responding to anti-TCR $\delta$ 1 stimulation were analyzed.

### IL-2 release and assay

Stimulation of TCR transfectants for IL-2 release was performed as described (38, 42). Briefly, 1  $\times$  10<sup>5</sup> transfectants were cultured with the indicated half-log dilution of the anti-TCR $\delta$ 1 mAb, stimulatory compounds, or tumor cells in the presence of 1  $\times$  10<sup>5</sup> glutaraldehyde-fixed Va2 cells (except for tumor cells) and 10 ng/ml PMA. After 24 h, supernatants were harvested and frozen at -20°C. For IL-2 assays, the supernatants were thawed and used at a one-eighth dilution to stimulate the proliferation of the IL-2-dependent cell line HT-2. The cultures were pulsed with 1  $\mu$ Ci [<sup>3</sup>H]thymidine (2 Ci/mmol) at 18 h and harvested 6 h later.

### Flow cytometric analysis

TCR transfectants were analyzed by one- or two-color immunofluorescence poststaining with the appropriate mAb as described (38). Cells were incubated with mouse mAbs on ice for 30 min, washed, and stained with PE-conjugated F(ab')<sub>2</sub> goat anti-mouse Ig antisera (Biosource, Camarillo, CA) for an additional 30 min on ice. After washing, the cells were resuspended in FACS buffer containing propidium iodide and analyzed by flow cytometry. Flow cytometry was performed with an FACScan flow cytometer (BD Biosciences, Palo Alto, CA), and the data were analyzed using FlowJo software (Tree Star, Ashland, OR).

### Modeling the human V $\gamma$ 2V $\delta$ 2 TCR

The DG.SF13 TCR is expressed by a synovial V $\gamma$ 2V $\delta$ 2 T cell clone isolated from a patient with rheumatoid arthritis (43). This receptor was used for our previous transfection and mutagenesis experiments on the V $\gamma$ 2V $\delta$ 2 TCR (26, 29), and its sequence has been published (26). The sequence of the DG.SF13 TCR varies from the G115 TCR that was crystallized (28), as

it has slightly different CDR3 regions. For comparison with other studies, numbering of amino acid residues is the same as used for G115 TCR. V $\gamma$ 2V $\delta$ 2 T cell clone sequences listed in Supplemental Table I are from Refs. 18, 27–29, 31, 38, 44–46. All figures were made with PyMOL X11 Hybrid (DeLano Scientific, South San Francisco, CA). Electrostatic surface potential was calculated with the APBS PyMOL plugin (DeLano Scientific) (47). In silico mutations were made in PyMol using the Mutagenesis Wizard (DeLano Scientific). The contact residues for other TCRs for MHC/CD1-peptide/lipid complexes were assessed for unconventional TCRs (48, 49), for conventional  $\alpha\beta$  TCRs specific for MHC class IIb complexes (50–65), and for conventional  $\alpha\beta$  TCRs specific for MHC class II complexes (66–71). The TCR structures shown are taken from the TCR-ligand complex. The TCRs are identically scaled using a PyMol script kindly provided by Dr. DeLano but the diagonal orientation does not attempt to match the docking angles on their MHC/CD1 ligands. Contact residues were colored as follows: those in CDR1  $\alpha/\delta$  are blue, CDR2  $\alpha/\delta$  are magenta, CDR3  $\alpha/\delta$  are yellow, CDR1  $\beta/\gamma$  are red, CDR2  $\beta/\gamma$  are orange, CDR3  $\beta/\gamma$  are green, and HV4  $\beta/\gamma$  are pink. Note that alternative terminology for human  $\gamma$ -chain exists: V $\gamma$ 2 is also termed V $\gamma$ 9 (TRGV9); J $\gamma$ 1.1 is also termed J $\gamma$ P1 (TRGJP1), J $\gamma$ 1.2 is also termed J $\gamma$ P (TRGJP), J $\gamma$ 1.3 is also termed J $\gamma$ 1 (TRGJ1), J $\gamma$ 2.1 is also termed J $\gamma$ P2 (TRGJP2), and J $\gamma$ 2.3 is also termed J $\gamma$ 2 (TRGJ2) (72). For discussions of murine  $\gamma\delta$  TCR, we use the nomenclature of Heilig and Tonegawa (73).

## Results

### Effects of CDR mutations in the V $\gamma$ 2 and V $\delta$ 2 chains on the reactivity of anti-TCR Abs

Although mutations of CDR loops are less likely to affect the overall folding of the V $\gamma$ 2V $\delta$ 2 TCR, we confirmed this by examining the reactivity of a panel of mAbs specific for the V $\gamma$ 2 and V $\delta$ 2 regions to mutated V $\gamma$ 2V $\delta$ 2 TCRs. None of the CDR mutations affected reactivity of the anti-TCR $\delta$ 1 mAb directed to the C $\delta$  region (Table I). Similarly, none of the mutation in CDR1 $\gamma$  affected reactivity by four anti-V $\gamma$ 2 mAbs. Mutations in Arg59 $\gamma$  (for 4D7) and Lys60 $\gamma$  (for 4D7 and 7A5) of the CDR2 $\gamma$  did abolish reactivity for two of the mAbs while maintaining reactivity to the two others (Table I). None of the CDR1 $\delta$  or CDR2 $\delta$  mutations affected reactivity of five mAbs specific for the V $\delta$ 2 region (Table I). We were unable to express the Lys53Ala mutation in the V $\delta$ 2 region despite several attempts, suggesting that this mutation does alter TCR folding or assembly. Thus, based on their continued reactivity with mAbs specific for the V $\gamma$ 2 and V $\delta$ 2 regions, our CDR mutations generally did not result in disruption in the conformation of the V $\gamma$ 2V $\delta$ 2 TCR.

### Essential residues in the CDR1 $\gamma$ and CDR2 $\gamma$ of the V $\gamma$ 2 chain

Because the CDR mutations did not cause major disruptions in V $\gamma$ 2V $\delta$ 2 TCR folding, we determined the effects of these CDR mutations on prenyl pyrophosphate Ag recognition. Four residues in CDR1 $\gamma$  and four residues in CDR2 $\gamma$  were mutated from polar hydrophilic amino acids to the nonpolar, hydrophobic amino acid alanine, except for Ile30Glu, in which the hydrophobic isoleucine residue was mutated to the negatively charged, hydrophilic amino acid aspartic acid (Table I). For these studies, mutants and wild-type transfectants were stimulated with HMBPP or with an anti-C $\delta$  mAb to serve as a positive control in the presence of Va2-presenting cells. Multiple transfectants derived from separate transfections were tested for each mutant to confirm each result.

As expected, the native DG.SF13 V $\gamma$ 2V $\delta$ 2 TCR maintained its responsiveness to HMBPP upon transfection into  $\beta^-$  Jurkat cells. For CDR1 $\gamma$  mutations, mutation of the exposed residue, Thr29, to alanine abolished recognition of HMBPP (Fig. 1). In contrast, mutation of three other residues (Ile30Glu, Thr33Ala, and Ser34Ala) that are in areas not as readily accessible for binding did not alter recognition. Binding of V $\gamma$ 2-specific mAbs was unaffected by these mutations (Table I). These results were verified by additional independently derived transfectants for each mutation (Supplemental Fig. 1). Additional residues (Ile28Val, Ala32Glu, and Val35Phe) that differ between human and rhesus monkey did not affect recognition because a chimeric TCR of rhesus monkey V $\gamma$ 2 chain paired with the human V $\delta$ 2 chain still recognized HMBPP presented by human APCs (38). The alanine to glutamic acid change at CDR1 $\gamma$  residue 32 is the only nonconservative change among the three residues.

The CDR2 $\gamma$  residues that were mutated include two (Tyr54 and Thr57) on the solvent-exposed portion of the CDR2 $\gamma$  loop near the CDR1 $\gamma$  loop. Mutation of either of these two residues to alanine (Tyr54Ala and Thr57Ala) abolished recognition of HMBPP (Fig. 1). In contrast, mutation of two basic residues (Arg59 and Lys60) did not. These residues are located at the end of the binding groove and form a positively charged region that could potentially bind to the negatively charged pyrophosphate moiety of prenyl pyrophosphates. Because mutation of these residues to the neutral amino acid, alanine, did not affect HMBPP recognition, we find no evidence for involvement by this region in Ag recognition (Fig. 1). However, these mutations did alter mAb binding, with both Arg59Ala and Lys60Ala mutations abolishing 4D7 mAb binding and

Table I. Summary of V $\gamma$ 2V $\delta$ 2 TCR mutations

TCR Region	Mutation		Anti-V $\gamma$ and Anti-V $\delta$ mAb Staining				
	Nucleic Acid	Amino Acid	Ti $\gamma$ A	7A5	360	4D7	
V $\gamma$ 2 chain							
CDR1 $\gamma$	ACA → GCA	T29A	+	+	+	+	
	ATT → GAG	I30E	+	+	+	+	
	ACA → GCA	T33A	+	+	+	+	
	TCT → GCC	S34A	+	+	+	+	
CDR2 $\gamma$	TAT → GCC	Y54A	+	+	+	+	
	ACT → GCA	T57A	+	+	+	+	
	AGA → GCA	R59A	+	+	+	–	
CDR3 $\gamma$	AAG → GCG	K60A	+	–	+	–	
	AAA → GCA	K108A	+	+	+	+	
			BB3	4G6	389	G1	TiV $\delta$ 2
V $\delta$ 2 chain							
CDR1 $\delta$	GAA → GCA	E28A	+	±	+	+	±
	ATC → GAG	I30E	ND	ND	ND	ND	ND
	AAC → GCC	N32A	+	+	+	+	+
CDR2 $\delta$	CGA → GCA	R51A	+	+	+	+	+
	GAA → GCA	E52A	+	+	+	+	+

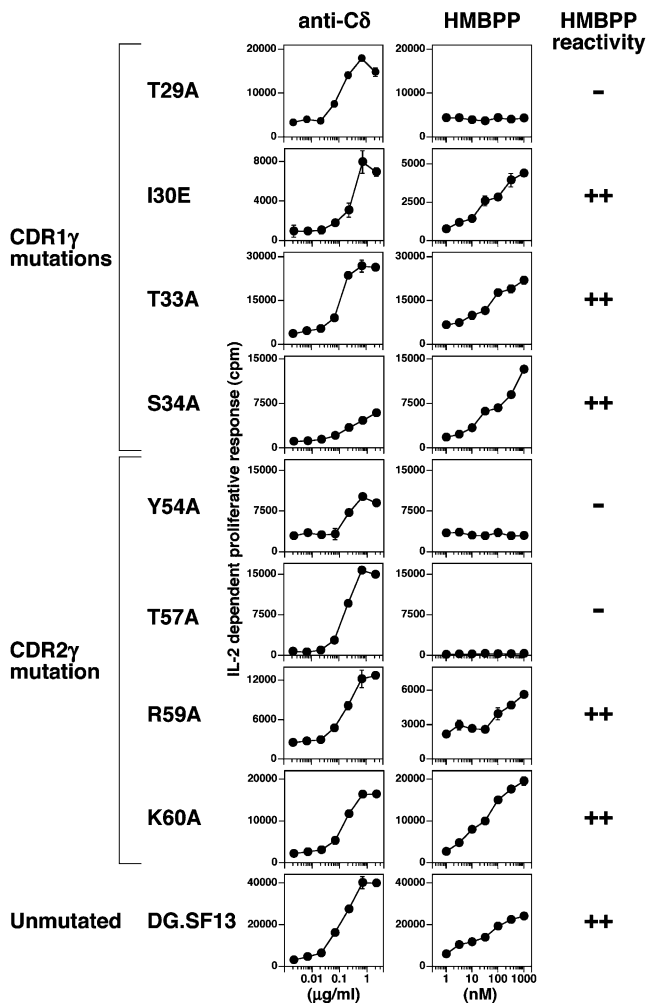


**FIGURE 1.** Recognition of HMBPP by V $\gamma$ 2V $\delta$ 2 TCR transfectants expressing mutant V $\gamma$ 2 chains. J.RT3-T3.5  $\beta^-$  Jurkat cells were transfected with unmutated or mutated DG.SF13 TCR- $\gamma$  cDNAs together with the unmutated DG.SF13 TCR  $\delta$ -chain cDNA. After drug selection, anti-C $\delta$  responsive transfectants were identified and stimulated with HMBPP in the presence of Va2 APCs and 2.5 ng/ml PMA. The anti-C $\delta$  mAb (anti-TCR $\delta$ 1) and HMBPP were added to the cultures starting at 2.15  $\mu$ g/ml and 1000 nM, respectively, and serially diluted by half-log intervals. After 24 h, the culture supernatants were harvested and assayed for IL-2 activity using the IL-2-dependent cell line HT2. Results from one transfectant are shown for each mutation and are representative of the results obtained with two to four other independently derived transfectants (Supplemental Fig. 1). Values shown are mean  $\pm$  SEM of duplicate or triplicate samples. HMBPP reactivity was considered (++) if the maximum HMBPP response was  $>40\%$  of the control anti-C $\delta$  response, (+) if between 20–40% of the control response, and (–) if  $<10\%$  of the control response.

with Lys60Ala also abolishing 7A5 mAb binding. Binding by the Ti $\gamma$ A and 360 mAbs was unaffected (Table I). Differences between human and rhesus monkey at residues Ser53Phe and Arg59Lys are conservative changes and did not affect recognition. The serine to phenylalanine mutation is located in a recessed area of the CDR2 $\gamma$  loop.

Thus, all of the mutations in CDR1 $\gamma$  and CDR2 $\gamma$  that alter HMBPP recognition are located in highly accessible, solvent exposed areas of the CDR loops of the V $\gamma$ 2V $\delta$ 2 TCR (28). In contrast, mutations that did not affect HMBPP recognition were located in recessed, less solvent exposed areas. Importantly, all three mutations that affected HMBPP response were distant (16–23 Å) from the proposed prenyl pyrophosphate-binding area that is composed mainly of residues from CDR3 $\gamma$  and CDR2 $\delta$ .

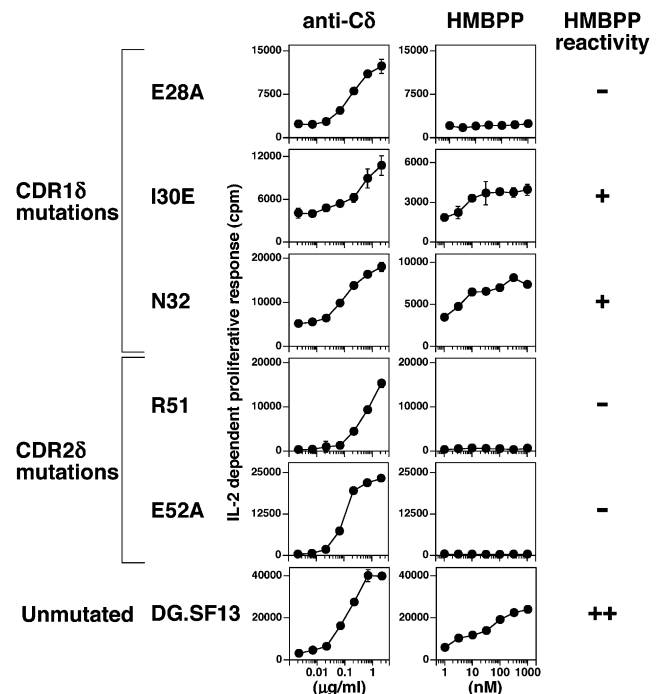


**FIGURE 2.** Recognition of HMBPP by V $\gamma$ 2V $\delta$ 2 TCR transfectants expressing mutant V $\delta$ 2 chains. J.RT3-T3.5  $\beta^-$  Jurkat cells were transfected with unmutated or mutated DG.SF13 TCR- $\delta$  cDNAs together with the unmutated DG.SF13 TCR  $\gamma$ -chain cDNA. Culture conditions and the IL-2 assay were as in Fig. 1. Results from one transfectant are shown for each mutation and are representative of the results obtained with one to four other independently derived transfectants (Supplemental Fig. 2).

#### *Essential residues in the CDR1 $\delta$ and CDR2 $\delta$ region of the V $\delta$ 2 chain*

To investigate the role of V $\delta$ -chain residues in nonpeptide Ag recognition, three residues in CDR1 $\delta$  and two residues in CDR2 $\delta$  were selected for mutation (Fig. 2). One of the three mutations in CDR1 $\delta$  affected the HMBPP recognition. The residue mutated, Glu28, is highly accessible but spaced 19–22 Å away from the proposed prenyl pyrophosphate-binding area. This mutation was nonconservative, with an alanine being substituted for a negatively charged glutamic acid residue (Fig. 2). The other mutations, Ile30Glu and Asn32Ala, did not affect recognition (Fig. 2).

Two mutations in the CDR2 $\delta$ , Arg51Ala and Glu52Ala, both affected recognition of HMBPP. The Arg51 and Glu52 residues are located within the proposed prenyl pyrophosphate-binding site (within 4–10 Å of Lys109 for Arg51 and 10–13 Å for Glu52). The loss of reactivity by mutating Arg51 confirms an earlier study in which mutation of Arg51 to either alanine or glutamic acid abolished recognition (30). Changing one residue in CDR2 $\delta$  outside of this area, Asp54, to glycine did not affect recognition because glycine is used at this position in the rhesus monkey V $\delta$ 2 chain, and a chimeric receptor of rhesus monkey V $\delta$ 2 paired with human V $\gamma$ 2 still recognized prenyl pyrophosphates (38). Note that this residue is located 11–15 Å away from the proposed binding site. These findings demonstrate that part but not all of CDR2 $\delta$  contributes to prenyl pyrophosphate recognition.

#### *Abrogation of Ag and tumor recognition by mutation of K108 in CDR3 $\gamma$*

We had earlier established the importance of the CDR3 $\gamma$  in prenyl pyrophosphate recognition by altering reactivity through mutation of its junctional region (29). We and others have proposed that

lysine residues in the J $\gamma$  region of CDR3 $\gamma$  combined with Arg51 in CDR2 $\delta$  constitute a potential binding site for the pyrophosphate residues of IPP and HMBPP because the positive charges on the amino groups are available for ionic bonding (27, 28, 30). In addition to prenyl pyrophosphates, there have been reports that the mitochondrial protein F1-ATPase expressed on tumor cells can be recognized by the V $\gamma$ 2V $\delta$ 2 TCR (74). To determine the importance of this proposed site in Ag and tumor recognition, we mutated one of these residues, Lys108, in the J $\gamma$ 1.2 segment of CDR3 $\gamma$  to alanine.

To study tumor reactivity reportedly due to F1-ATPase (74), we determined reactivity of the wild-type V $\gamma$ 2V $\delta$ 2 TCR and the Lys108Ala TCR mutant for the stimulatory plasmacytoma, RPMI 8226. Whereas the unmutated TCR transfectant responded to the RPMI 8226, but not to the control Raji cell line, mutation of Lys108 abrogated reactivity to RPMI 8226 (Fig. 3, right bottom panel).

Similarly, mutation of Lys108 completely abrogated recognition of HMBPP (Fig. 3) while preserving stimulation by an anti-C $\delta$  mAb.

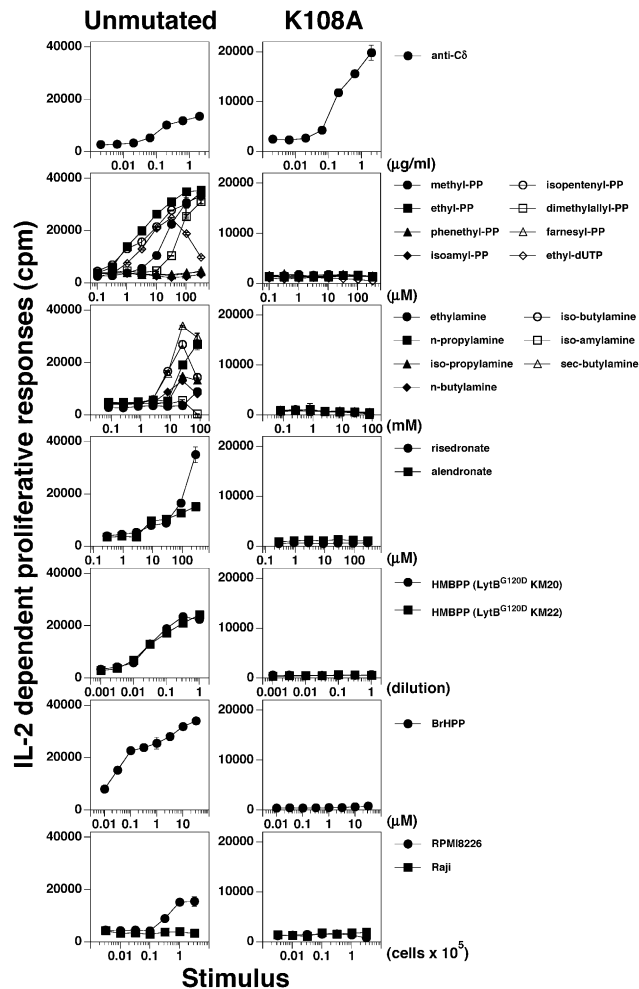


**FIGURE 3.** Critical role of K108 in the CDR3 of V $\gamma$ 2 in the recognition of nonpeptide Ags and tumor cells. JRT3-T3.5  $\beta$ <sup>-</sup> Jurkat cells were transfected with the DG.SF13 TCR  $\gamma$ -chain cDNA with a lysine (K) to alanine (A) mutation at position 108 in the CDR3 $\gamma$  region and the unmutated DG.SF13 TCR- $\delta$  cDNA. The transfectant obtained was named K108A and compared with an unmutated DG.SF13 TCR transfectant for stimulation by anti-C $\delta$ , prenyl pyrophosphates, alkylamines, bisphosphonates (risedronate and alendronate), HMBPP (in supernatants of the *E. coli* *lytB* mutants, KM20, and KM22), bromohydrin pyrophosphate, and lymphoma cell lines (RPMI 8226 and Raji). Culture conditions and the IL-2 assay were as in Fig. 1.

This mutation also abrogated direct stimulation by five other prenyl pyrophosphates (Fig. 3). Other stimulatory compounds, such as bisphosphonates and alkylamines, stimulate V $\gamma$ 2V $\delta$ 2 T cells indirectly by blocking the enzyme FPP synthase, causing increases in cellular IPP levels (13, 14). Consistent with IPP being the direct stimulating Ag, the Lys108Ala mutation also abrogated stimulation by six alkylamines and two bisphosphonates (Fig. 3). These results confirm an earlier report in which Lys108Ala, Lys108Glu, and Lys109Glu mutations (but not Lys109Ala) abolished recognition of prenyl pyrophosphate, bisphosphonate, and alkylamine stimulatory compounds (30, 31).

The loss of reactivity to the stimulatory compounds and the tumor cell line by the Lys108Ala mutation suggests that there are shared structural features for these Ags (including the Ag expressed on the RPMI 8226 plasmacytoma).

#### Narrow length distribution of CDR3 $\gamma$ in V $\gamma$ 2J $\gamma$ 1.2 chains but not in V $\gamma$ 2J $\gamma$ 1.3/2.3 chains

To determine if there were any length restrictions or common motifs in the CDR3 $\gamma$  junctional region of reactive V $\gamma$ 2V $\delta$ 2 T cells, we examined reported sequences of 107 reactive and nonreactive V $\gamma$ 2V $\delta$ 2 T cell clones (Supplemental Table I). The J $\gamma$ 1.2 segment was highly favored being used by 84 out of 90 (93%) reactive clones. The length of CDR3 $\gamma$  in V $\gamma$ 2J $\gamma$ 1.2 chains was also highly restricted, with 98% of T cell clones with CDR3 $\gamma$  lengths of  $\pm$ 2 residues. There were no major differences in CDR3 $\gamma$  length between reactive and nonreactive clones (Supplemental Fig. 3). However, because TCR differences between reactive and nonreactive clones could be mapped to the CDR3 $\delta$  region in some cases (Table II), at least some of the V $\gamma$ 2 chains expressed by nonreactive clones would be reactive if paired with a reactive V $\delta$ 2 chain.

Many clones (18 out of 84, 21%) used the invariant V $\gamma$ 2J $\gamma$ 1.2 aa sequence (75) either due to germline gene rearrangement or the addition of junctional residues with trimming of the germline V $\gamma$ 2 and J $\gamma$ 1.2 segments (Supplemental Table I). This frequency of invariant V $\gamma$ 2J $\gamma$ 1.2 chains is consistent with that reported for peripheral blood V $\gamma$ 2V $\delta$ 2 T cells (75). In most of the noninvariant V $\gamma$ 2J $\gamma$ 1.2 chains, there were only one to two junctional residues (with a maximum of four) with corresponding losses in the germline V $\gamma$ 2 and J $\gamma$ 1.2 segments to preserve CDR3 $\gamma$  length. Thus, all of the V $\gamma$ 2J $\gamma$ 1.2 chains had germline amino acid sequences for much or all of the CDR3 $\gamma$  region. When junctional residues were added, they favored basic lysine and arginine residues, with 25 out of 66 (38%) reactive V $\gamma$ 2J $\gamma$ 1.2 chains having at least one basic residue added. Also, none of the TCRs had deletion of the Lys108 or Lys109 residues. The glutamic acid located at position 105 is not required for reactivity because it is absent in some human V $\gamma$ 2J $\gamma$ 1.2 chains (Supplemental Table I) and in rhesus monkey V $\gamma$ 2, which is able to recognize HMBPP presented by human APCs when paired with human V $\delta$ 2 (Table II) (38).

In contrast to V $\gamma$ 2J $\gamma$ 1.2 chains, a high proportion of V $\gamma$ 2V $\delta$ 2 T cell clones using V $\gamma$ 2J $\gamma$ 1.3/2.3 chains were nonreactive to prenyl pyrophosphates (46% nonreactive versus 14% nonreactive for V $\gamma$ 2J $\gamma$ 1.2 chains). Moreover, the V $\gamma$ 2J $\gamma$ 1.3/2.3 chains had shorter chain lengths (6–14 residues versus 11–14 residues for V $\gamma$ 2J $\gamma$ 1.2 chains) with higher variability in length. This shorter length may be optimal for reactivity because a short V $\gamma$ 2J $\gamma$ 1.3 chain (eight residues) using a GN junctional sequence paired with the DG.SF13 V $\delta$ 2 chain was responsive to HMBPP but a longer mutant V $\gamma$ 2J $\gamma$ 1.2 (12 residues) chain, in which the GN residues were substituted for a W residue, was unresponsive when paired with the same DG.SF13 V $\delta$ 2 chain (Table II).

Table II. Diversity of CDR3 $\gamma$  or CDR3 $\delta$  sequences in V $\gamma$ 2V $\delta$ 2 T cells expressing an identical V $\gamma$ 2 or V $\delta$ 2 chain

Clone/ Transfectant	V $\gamma$ 2	N	J $\gamma$	J $\gamma$	V $\delta$ 2	(aa 97)	N/D/N	J $\delta$	J $\delta$	CDR3 $\delta$ Length	Reactivity	
AC2 <sup>a</sup>	LWEV		QELGKKIK	J $\gamma$ 1.2	CDT	<b>T</b>	GG	SWDTRQM	J $\delta$ 3	13	+	
AC8 <sup>a</sup>	LWEV		QELGKKIK	J $\gamma$ 1.2	CDT	<b>W</b>	G	SWDTRQM	J $\delta$ 3	13	+	
G1 <sup>b</sup>	LWEV		QELGKKIK	J $\gamma$ 1.2	CD	<b>R</b>	V PP	STGD	TDKL	J $\delta$ 1	14	+
G2 <sup>b</sup>	LWEV		QELGKKIK	J $\gamma$ 1.2	CDT	<b>V</b>	NADAEN		DKL	J $\delta$ 1	13	+
G3 <sup>b</sup>	LWEV		QELGKKIK	J $\gamma$ 1.2	CD	<b>A</b>	V LGDTSRP		DKL	J $\delta$ 1	14	+
G4 <sup>b</sup>	LWEV		QELGKKIK	J $\gamma$ 1.2	CD	<b>L</b>	V LGVNTG		WDTRQM	J $\delta$ 3	16	+
M3 <sup>b</sup>	LWEV		QELGKKIK	J $\gamma$ 1.2	CD	<b>W</b>	L LGDTV		TDKL	J $\delta$ 1	13	+
G5 <sup>b</sup>	LWEV		QELGKKIK	J $\gamma$ 1.2	CDT	<b>G</b>	GYAN		WDTRQM	J $\delta$ 3	14	+
G6 <sup>b</sup>	LWEV		QELGKKIK	J $\gamma$ 1.2	CDT	<b>V</b>	EA		LTAQL	J $\delta$ 2	11	+
M4 <sup>b</sup>	LWEV		QELGKKIK	J $\gamma$ 1.2	CD	<b>N</b>	W GDKM		TAQL	J $\delta$ 2	12	+
T2 <sup>b</sup>	LWEV		QELGKKIK	J $\gamma$ 1.2	CD	<b>N</b>	T GGY		SWDTRQM	J $\delta$ 3	15	+
T3 <sup>b</sup>	LWEV		QELGKKIK	J $\gamma$ 1.2	CDT	<b>V</b>	LGDS		SWDTRQM	J $\delta$ 3	15	+
T4 <sup>b</sup>	LWEV		QELGKKIK	J $\gamma$ 1.2	CD	<b>I</b>	L GDAA		LTAQ	J $\delta$ 2	12	+
T5 <sup>b</sup>	LWEV		QELGKKIK	J $\gamma$ 1.2	CDT	<b>I</b>	LGDT		WDTRQM	J $\delta$ 3	14	+
T6 <sup>b</sup>	LWEV		QELGKKIK	J $\gamma$ 1.2	CDT	<b>L</b>	PLGAKGY		DKL	J $\delta$ 1	14	+
T7 <sup>b</sup>	LWEV		QELGKKIK	J $\gamma$ 1.2	CDT	<b>V</b>	SGDTH		SWDTRQM	J $\delta$ 3	16	+
M12 <sup>b</sup>	LWEV		ELGKKIK	J $\gamma$ 1.2	CD	<b>S</b>	L LTSQLSLGDH		TDKL	J $\delta$ 1	18	+
M6 <sup>b</sup>	LWEV		ELGKKIK	J $\gamma$ 1.2	CD	<b>T</b>	G FRGKDT		WDTRQM	J $\delta$ 3	17	+
T22 <sup>b</sup>	LWEV		ELGKKIK	J $\gamma$ 1.2	CD	<b>K</b>	S AGNP		SWDTRQM	J $\delta$ 3	15	-
C.15	LWE	A	QELGKKIK	J $\gamma$ 1.2	CDT	<b>L</b>	GSGGSAER		TDKL	J $\delta$ 1	12	+
I.7	LWE	A	QELGKKIK	J $\gamma$ 1.2	CDT	<b>P</b>	GIGYT		WDTRQM	J $\delta$ 3	15	-
$\gamma$ 001/ $\delta$ 263 <sup>c</sup>	LWEV		QELGKKIK	J $\gamma$ 1.2	CDT	<b>I</b>	LGD		TDKL	J $\delta$ 1	10	+
$\gamma$ 001/ $\delta$ 016 <sup>c</sup>	LWEV		QELGKKIK	J $\gamma$ 1.2	CDT	<b>V</b>	EGMRRNLLGERGSY		TDKL	J $\delta$ 1	22	+
$\gamma$ 001/ $\delta$ 255 <sup>c</sup>	LWEV		QELGKKIK	J $\gamma$ 1.2	CDT	<b>P</b>	MRAPDWGTLGN		TDKL	J $\delta$ 1	19	-
PBL $\gamma$ /DG $\delta$ <sup>d</sup>	LWE	GN	YKK	J $\gamma$ 1.3	CDT	<b>L</b>	VS		TDKL	J $\delta$ 1	10	+
mutDG $\gamma$ /DG $\delta$ <sup>d</sup>	LWE	<u>GN</u>	ELGKKIK	J $\gamma$ 1.2	CDT	<b>L</b>	VS		TDKL	J $\delta$ 1	10	-
DG.SF13	LWE	<u>W</u>	ELGKKIK	J $\gamma$ 1.2	CDT	<b>L</b>	VS		TDKL	J $\delta$ 1	10	+
DG $\gamma$ /monkey $\delta$ <sup>e</sup>	LWE	W	ELGKKIK	J $\gamma$ 1.2	SD	<b>H</b>	I LEGGIRG		TDKL	J $\delta$ 1	13	+
Monkey $\gamma$ <sup>f</sup> /DG $\delta$	LWEV	Q	QFGRKVK	J $\gamma$ 1.2	CDT	<b>L</b>	VS		TDKL	J $\delta$ 1	10	+
G115/G9 <sup>f</sup>	LWE	AQ	QELGKKIK	J $\gamma$ 1.2	CD	<b>T</b>	L GMGGEY		TDKL	J $\delta$ 1	13	+

Horizontal dividers separate groups of TCRs that share either identical V $\gamma$ 2 or V $\delta$ 2 chains but that differ in the other chain and, in some cases, in prenyl pyrophosphate reactivity. Position 97 in the V $\delta$ 2 chains is bolded and its position indicated in the column title. Likely sequence differences causing loss of reactivity are underlined. Note that alternative names for V $\gamma$ 2, J $\gamma$ 1.2, and J $\gamma$ 1.3 are V $\gamma$ 9 (TRGV9), J $\gamma$ P (TRGJP), and J $\gamma$ 1 (TRGJ1).

<sup>a</sup>Sequences from T cell clones (18).

<sup>b</sup>Sequences from T cell clones, reactivity reported in Ref. 44.

<sup>c</sup>Sequences from T cell transfectants, reactivity reported in Ref. 31.

<sup>d</sup>Sequences from T cell transfectants, reactivity reported in Ref. 29.

<sup>e</sup>Sequences from T cell transfectants, reactivity reported in Ref. 38.

<sup>f</sup>Sequences from G115/G9 T cell clone used for crystal structure, reactivity reported in Ref. 28.

### Conserved hydrophobic residue at position 97 but variable CDR3 $\delta$ length and sequence

CDR3 $\delta$  regions are the most variable junctional region in mammals due to the availability of multiple V, D, and J gene segments for rearrangement and due to the ability of multiple D segments to rearrange in tandem and in any reading frame (76). In mice, the CDR3 $\delta$  region has been shown to be critical for  $\gamma\delta$  T cell recognition of T10 and T22 MHC class Ib molecules. A 9 aa conserved loop motif in the CDR3 $\delta$  region inserts into a cavity on the T10 molecule and provides most of contact residues and 67% of the interface. To determine if a similar motif could be identified in the CDR3 $\delta$  region of V $\gamma$ 2V $\delta$ 2 TCR, we examined the sequences of 107 reactive and nonreactive V $\gamma$ 2V $\delta$ 2 T cell clones (Supplemental Table I).

Unlike its V $\gamma$ 2 chain partner, the length of the CDR3 of the V $\delta$ 2 chain varied widely, ranging from 10 to 18 aas, while retaining responsiveness to prenyl pyrophosphates (Supplemental Fig. 3, Supplemental Table I). Moreover, unlike V $\gamma$ 2 chains in which there are critical residues in the J $\gamma$  segment and a preference for J $\gamma$ 1.2, the V $\delta$ 2 chain can use J $\delta$ 1, J $\delta$ 2, or J $\delta$ 3 and retain responsiveness despite significantly different sequences and lengths. The longer and more variable length of the CDR3 $\delta$  segment is a general characteristic of  $\delta$ -chains (77).

Although the length of CDR3 $\delta$  is variable, there is a strong preference for a hydrophobic residue at position 97. Ninety-two percent of V $\delta$ 2 chains (61 out of 71) from reactive T cell clones used a hydrophobic residue at this position versus 53% (8 out of 15) of V $\delta$ 2 chains from nonreactive T cell clones. No reactive clone used proline, lysine, or arginine at this position (Supplemental Table I). There are examples of clones with identical V $\gamma$ 2 chains but different V $\delta$ 2 chains in which loss of reactivity can be correlated with a nonhydrophobic residue at position 97 (Table II). In these cases, the nonreactive V $\gamma$ 2V $\delta$ 2 T cell clone has either a polar serine amino acid at this position (for the nonreactive T22 clone versus the reactive M6/M12 clones) or the kinked proline amino acid (for the nonreactive I.7 clone compared with the reactive C.15 clone). Similarly, transfection of a V $\gamma$ 2 chain ( $\gamma$ 001) paired with a V $\delta$ 2 chain ( $\delta$ 255) with a proline at this position did not confer reactivity to prenyl pyrophosphates, although two other V $\delta$ 2 chains ( $\delta$ 263 and  $\delta$ 016) with hydrophobic residues did (31). Mutation of Leu<sup>97</sup> to either alanine or serine abolished prenyl reactivity (31), confirming its importance.

Whereas position 97 was mainly restricted to hydrophobic amino acids, the residues prior to and after 97 were quite diverse, including both positively and negatively charged amino acids as well

Table III. Effect of V $\gamma$ 2V $\delta$ 2 TCR mutations and rhesus monkey polymorphisms on prenyl pyrophosphate reactivity

TCR Region	Polymorphism Between Human and Rhesus Monkey <sup>a</sup>	Mutation of Human V $\gamma$ 2V $\delta$ 2 TCR	Prenyl Pyrophosphate Reactivity	Reference	
V $\gamma$ 2 chain	CDR1 $\gamma$	I28V	+	(38)	
			T29A	-	Current paper
			I30E	+	Current paper
		A32E		+	(38)
			T33A	+	Current paper
			S34A	+	Current paper
	CDR2 $\gamma$	V35I		+	(38)
		S53F		+	(38)
			Y54A	-	Current paper
			T57A	-	Current paper
			R59K	+	(38)
	CDR3 $\gamma$		R59A	+	Current paper
			K60A	+	Current paper
			W104GN	-	(29)
				+	(38)
			+	(38)	
			+	(38)	
		K108A	-	Current paper and (31)	
		K108E	-	(30)	
	K109A	+	(31)		
	K109E	-	(30)		
V $\delta$ 2 chain	CDR1 $\delta$		E28A	-	Current paper
			I30E	+	Current paper
		G31S		+	(38)
			R51A	-	Current paper and (31)
			R51E	-	(31)
			E52A	-	Current paper
	CDR3 $\delta$	D54G		+	(38)
		C94S		+	(38)
			L97A	-	(31)
			L97S	-	(31)
			-	(31)	

<sup>a</sup>Reactivity of rhesus monkey V gene segments was assessed by pairing with the corresponding partner human V gene segments and transfecting into J.RT3-T3.5  $\beta^-$  Jurkat followed by stimulation with Ags presented by human APCs as described (38).

as proline (Supplemental Table I). Moreover, there were no other clearly defined motifs in the N-, D $\delta$ -, or J $\delta$ -encoded portions of CDR3 $\delta$  that are required for reactivity. Thus, beyond a strong preference for a hydrophobic residue at position 97, no other motif can be found within CDR3 $\delta$  that correlates with reactivity. Taken together, the diverse length and amino acid composition of CDR3 $\delta$  from reactive V $\gamma$ 2V $\delta$ 2 T cell clones suggests that optimal prenyl pyrophosphate reactivity requires a hydrophobic residue at position 97 but is tolerant to a wide variety of sequences in and lengths of the N, D, and J regions.

#### Model of V $\gamma$ 2V $\delta$ 2 TCR contact residues in relation to the proposed prenyl pyrophosphate-binding site

The structures of human G115 V $\gamma$ 2V $\delta$ 2 TCR (Fig. 4) and murine G8 V $\gamma$ 4V $\alpha$ / $\delta$ 11.3 TCR show more protrusions and clefts in the binding face of the TCR (48, 78) compared with the flatter surfaces of  $\alpha\beta$  TCRs specific for peptide-MHC class I/II complexes. The CDRs of the V $\gamma$ 2V $\delta$ 2 TCR protrude (Fig. 4A). CDR3 $\gamma$  and CDR3 $\delta$  are especially prominent, creating a cleft between the two CDRs. There are two positively charged regions in this cleft (shaded blue) (Figs. 4D, 4F, 6), one positioned near the base of CDR3 $\delta$  formed by Lys109 $\gamma$  from J $\gamma$ 1.2 and Arg51 $\delta$  from CDR2 $\delta$  and a second located on the other side of the cleft formed by Arg59 $\gamma$  and Lys60 $\gamma$  from CDR2 $\gamma$ .

Mutation of residues in the second positively charged region formed by Arg59 $\gamma$  and Lys60 $\gamma$  from CDR2 $\gamma$ , although abolishing binding by some anti-V $\gamma$ 2 mAbs (Table I), did not affect prenyl

pyrophosphate recognition (Table III), arguing against the involvement of this second positively charged region. In contrast, alanine mutation of Lys108 (Fig. 3) and Lys109 (30) that is located in the first positively charged region closest to the Leu97 residue in CDR3 $\delta$  completely abrogated recognition of all prenyl pyrophosphates studied. Alanine mutation of Lys108 also abolished bisphosphonate and alkylamine recognition. Importantly, recognition of the plasmacytoma, RPMI 8226, was also lost. This result suggests that the Ag recognized by V $\gamma$ 2V $\delta$ 2 T cells in RPMI 8226 is IPP or another prenyl pyrophosphate and not F1-ATPase because these two Ags have grossly different structures and would be expected to use different contact residues. However, F1-ATPase could function as a presenting molecule, although we have found no evidence for this (data not shown).

This first positively charged region is positioned immediately adjacent to the conserved hydrophobic amino acid at position 97 of CDR3 $\delta$  and has potential contributions from Lys108 $\gamma$ , Lys109 $\gamma$ , and Lys111 $\gamma$  from J $\gamma$ 1.2 and Arg51 $\delta$  from CDR2 $\delta$  (Fig. 4D, 4F). However, in silico mutagenesis and calculation of the surface potential suggests that most of the positive potential in the region is from Arg51 $\delta$  with some contribution from Lys109 $\gamma$ , but little or no contribution from Lys108 $\gamma$  and Lys111 $\gamma$  (Fig. 5). Consistent with this analysis, mutation of Lys109 $\gamma$  to alanine reduced but did not abolish prenyl pyrophosphate recognition (31), whereas mutation of Arg51 $\delta$  to alanine completely abolished recognition. We now show that the acidic amino acid Glu52 $\delta$ , from CDR2 $\delta$  that is near but outside the binding pocket, is also required for recognition. The



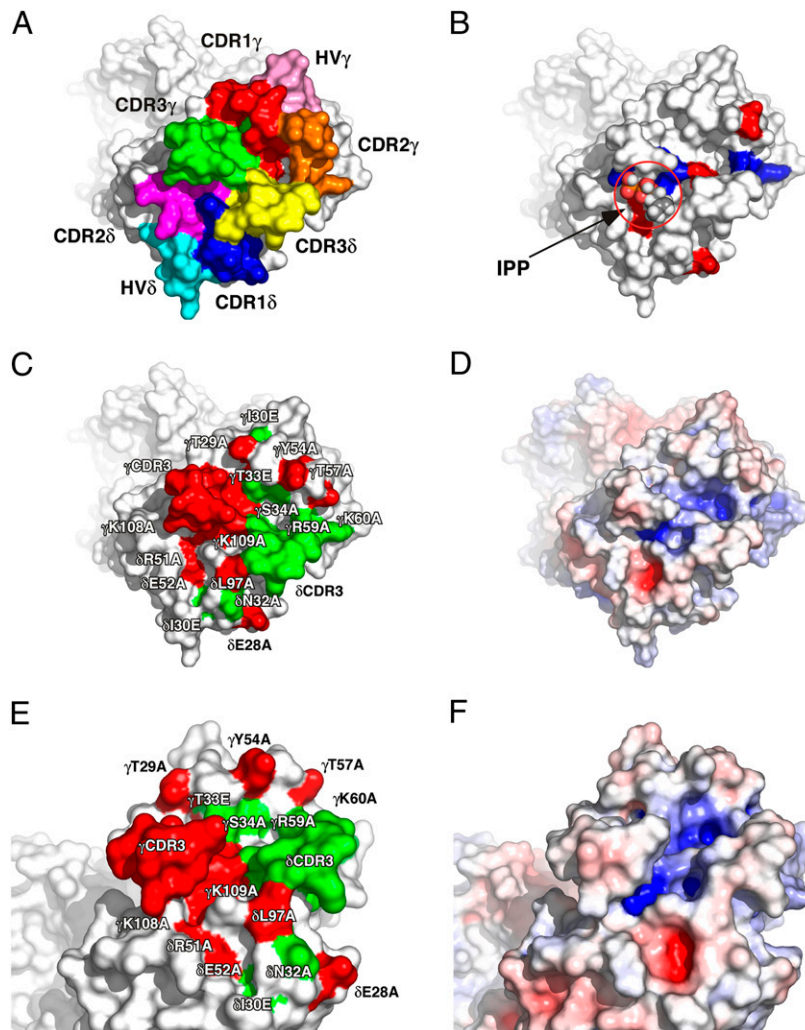


**FIGURE 4.** Recognition of prenyl pyrophosphates by human V $\gamma$ 2V $\delta$ 2 TCR is dependent on all CDRs. *A*, Top-down view of the V $\gamma$ 2V $\delta$ 2 TCR with CDRs for the  $\gamma$ - and  $\delta$ -chains labeled. CDR residues are colored such that those in CDR1 $\delta$  are blue, CDR1 $\delta$  are magenta, CDR3 $\delta$  are yellow, HV4 $\delta$  are cyan, CDR1 $\gamma$  are red, CDR2 $\gamma$  are orange, CDR3 $\gamma$  are green, and HV4 $\gamma$  are pink. *B*, Top-down view of the V $\gamma$ 2V $\delta$ 2 TCR with basic amino acids colored blue and acidic amino acids colored red. IPP is shown in the potential prenyl pyrophosphate-binding site for size comparison. *C*, Top-down view of critical amino acid residues that disrupt prenyl pyrophosphate recognition are colored red on the V $\gamma$ 2V $\delta$ 2 TCR, whereas noncritical amino acid residues are colored green. *D*, Top-down view of the surface potential of the V $\gamma$ 2V $\delta$ 2 TCR (colored from red [−8 kT] to blue [+8 kT]) reveals two positively charged potential binding sites. *E*, Side view of critical amino acid residues that disrupt prenyl pyrophosphate recognition are colored red on the V $\gamma$ 2V $\delta$ 2 TCR, whereas noncritical amino acid residues are colored green. *F*, Side view of the surface potential of the V $\gamma$ 2V $\delta$ 2 TCR (colored as in *D*).

area is a potential prenyl pyrophosphate-binding site because the positively charged amino acids can form ionic bonds to the negatively charged pyrophosphate moiety on IPP or HMBPP. The alkenyl chain could be positioned over the hydrophobic amino acid at position 97. Most proteins that bind phosphate(s) use either this mechanism of binding or use negatively charged amino acids to form an ionic bond to one of the positive charges on a divalent cation, leaving the second free to bind to the negative charges on the phosphate group. However, there is no evidence for direct high-affinity binding of prenyl pyrophosphates to the V $\gamma$ 2V $\delta$ 2 TCR either by equilibrium dialysis (C.T. Morita, unpublished observations) or soaking V $\gamma$ 2V $\delta$ 2 TCR crystals in IPP or HMBPP (28).

When the mutated CDR residues are localized on the V $\gamma$ 2V $\delta$ 2 TCR structure (critical residues colored red and noncritical residues colored green, Table III), a potential binding footprint of the TCR to its ligand is delineated (Fig. 4C, 4E). This area is much larger than the size of IPP or HMBPP (IPP and HMBPP are 10.3 Å and 10.9 Å in extended conformation, respectively) and encompasses more than just the prenyl pyrophosphate-binding site (Fig. 4B, 4D, 4F). Moreover, although both abolish recognition, Thr29 in CDR1 $\gamma$  is 34 Å from Glu28 in CDR1 $\delta$ . Similarly, Lys109 in CDR3 $\gamma$  is 15.3 Å from Thr29 in CDR1 $\gamma$  and 20.1 Å from Glu28 in CDR1 $\delta$ ; again, much larger distances than the size of a prenyl pyrophosphate. Thus, the footprint of V $\gamma$ 2V $\delta$ 2 TCR residues required for prenyl pyrophosphate recognition is significantly larger than the proposed prenyl pyrophosphate-binding site.

## Discussion

In this study, we show that mutations in all CDRs of the V $\gamma$ 2V $\delta$ 2 TCR can affect recognition of prenyl pyrophosphates. Mutation of highly accessible amino acids in CDR1 $\gamma$ , CDR2 $\gamma$ , and CDR1 $\delta$  loops all can abolish recognition, whereas mutations localized on the sides of the loops do not. Unlike TCR recognition by the two other unconventional innate T cells in which the contact residues are defined, there is no evidence that an extended D $\alpha$ / $\delta$  or J $\alpha$ / $\delta$  amino acid motif is required for recognition. Instead, there is a preference for a single hydrophobic, aliphatic amino acid at position 97 of CDR3 $\delta$  as previously reported (31, 79), but no restriction on: 1) the type of amino acid immediately preceding or following position 97; 2) the overall length of the CDR3 $\delta$  loop; or 3) other sequences in the D/N or J portions of the CDR3 $\delta$  loop. In contrast, the length of CDR3 $\gamma$  shows low variability, basic amino acids are preferred in its N region, and the J $\gamma$ 1.2 segment is preferentially used. Basic amino acids (Lys108 and Lys109) in the J $\gamma$  segment, the basic Arg51 and acidic Glu52 residues in the CDR2 $\delta$ , and the aliphatic amino acid at position 97 in CDR3 $\delta$  are all important for recognition and are located in or near a proposed prenyl pyrophosphate-binding site. Taken together, these results show that a large portion of the V $\gamma$ 2V $\delta$ 2 TCR is required for prenyl pyrophosphate recognition.

How well do alanine mutations predict residues in T cell Ag receptors that contact Ag or their presenting molecule? In three studies,  $\alpha\beta$  TCR contact residues for peptide-MHC class I ligands

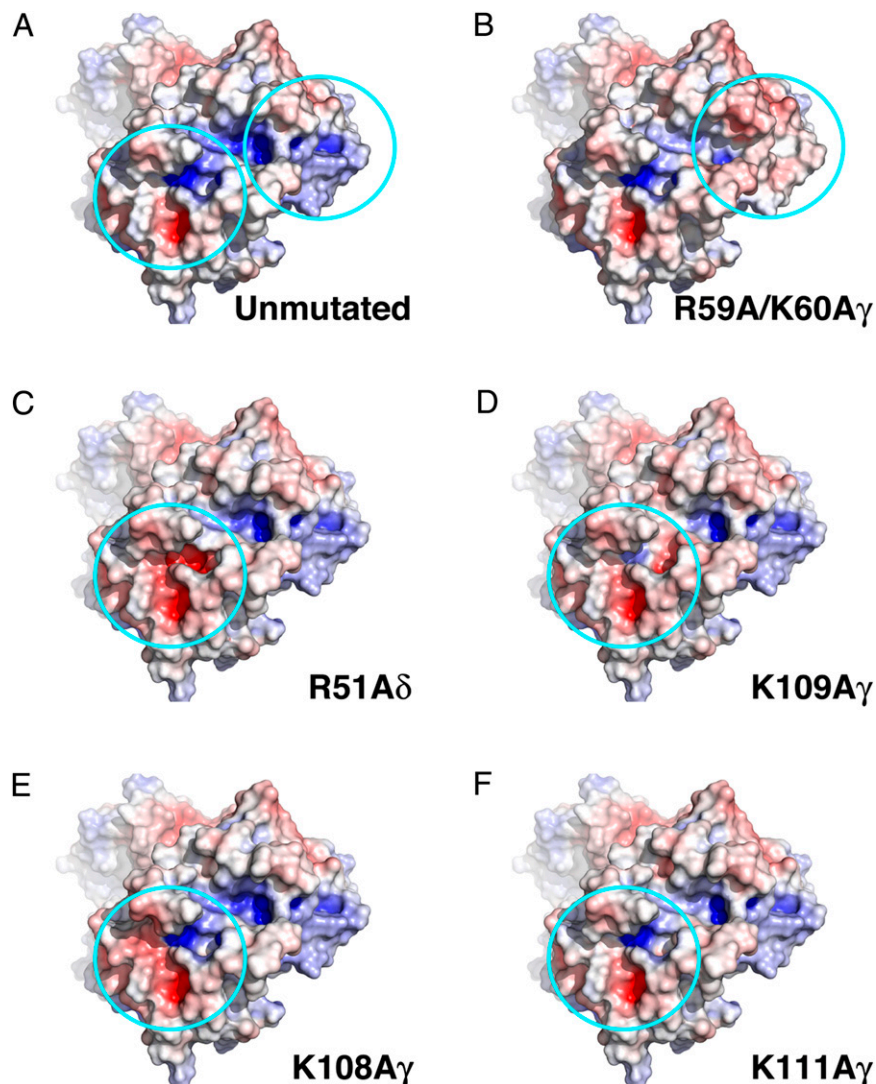


**FIGURE 5.** Surface potential effect of *in silico* alanine mutations of basic residues in the V $\gamma$ 2V $\delta$ 2 TCR. Basic residues were mutated to alanine *in silico* using PyMol (DeLano Scientific), and the surface potential of the mutated TCRs were calculated using the APBS plugin in PyMol. The TCRs are oriented with the  $\gamma$ -chains on the *top left* and the  $\delta$ -chains on the *bottom right* of the panels. Top-down views of the surface potential of the V $\gamma$ 2V $\delta$ 2 TCR are shown (colored from red [-8 kT] to blue [+8 kT]). The two positively charged regions are circled. *A*, Surface potential for the unmutated V $\gamma$ 2V $\delta$ 2 TCR. *B–F*, Effect on surface potential of alanine replacement of R59A and K60A $\gamma$  (*B*), R51A $\delta$  (*C*), K109A $\gamma$  (*D*), K108A $\gamma$  (*E*), and K111A $\gamma$  (*F*).

were determined from crystal structures. CDR contact and non-contact residues were then mutated to alanine and the mutant TCRs tested for binding to their respective peptide-MHC class I ligands. Mutation of contact residues to alanine reduced MHC/peptide ligand binding for 81% (17 out of 21) of the contact residues in the LC13 TCR (80), for 70% (7 out of 10) in the 2C TCR (81), and for 59% (13/22) in the JM22 TCR (82). Noncontact residues in CDRs containing contact residues also decreased binding, albeit, as might be expected, at lower rates (39%, 7 out of 18, for the LC13 TCR and 60%, 9 out of 15, for the 2C TCR). Importantly, none of 12 mutations in the  $\alpha$  and  $\beta$  hypervariable four-regions of the 2C TCR affected binding (none were contact residues). Most mutations that grossly affected structure were not expressed (only 1 out of 40 in LC13 (80), 9 out of 51 in 2C (81), and 0 out of 12 in JM22) (82). Thus, most mutations (70% overall) in CDR contact residues greatly reduce binding, whereas mutations in HV4 loops that did not contain contact residues had no effect. From these results, we would predict that mutations that abolish recognition likely identify either contact residues for the Ag/presenting molecule or noncontact residues in loops that contain contact residues. Our finding that residues well outside the proposed prenyl pyrophosphate-binding site affect recognition suggests that a larger molecule binds and presents these small molecules.

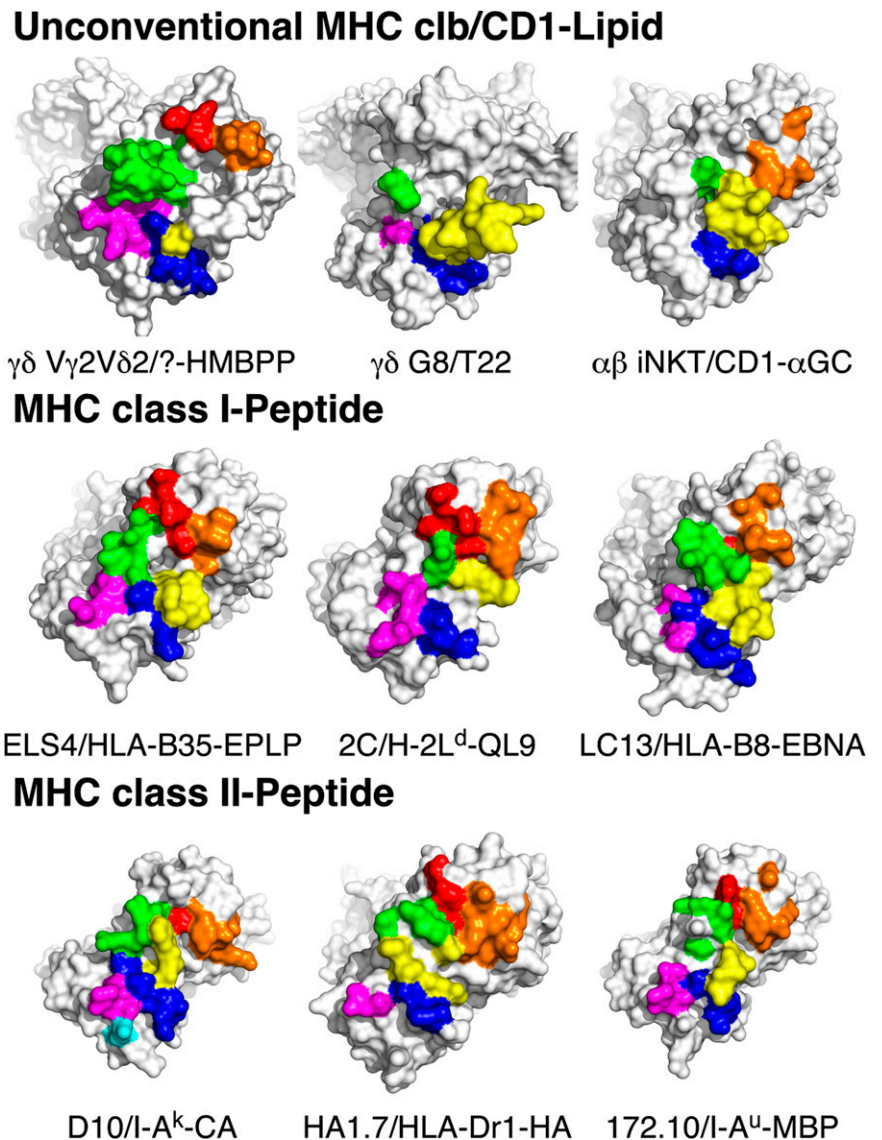
#### *Unconventional innate versus conventional peptide-MHC TCR recognition by T cells*

Although expressing rearranging TCRs, innate T cells, such as  $\gamma\delta$  T cells and iNKTs, likely play roles that more closely resemble those of innate myeloid cells. In keeping with their unique roles in the immune system, innate T cells commonly express TCRs that use germline encoded portions of the TCR to either recognize nonpeptide Ags presented by MHC class Ib or CD1 molecules or to directly recognize MHC class I-like molecules. Many  $\gamma\delta$  T cell populations, such as murine dendritic epidermal  $\gamma\delta$  T cells (83), express TCR with invariant receptors.  $\alpha\beta$  iNKTs that recognize self and foreign glycolipids presented by CD1d also express a semi-invariant TCR composed of a conserved V $\alpha$ J $\alpha$ -chain paired with a limited set of V $\beta$ -chains (84).

There are only two examples of unconventional TCR recognition by innate T cells that have been characterized at the molecular level to compare with V $\gamma$ 2V $\delta$ 2 TCR recognition of prenyl pyrophosphates. The only example for  $\gamma\delta$  T cells is the structure of a murine  $\gamma\delta$  TCR, G8, bound to the MHC class Ib molecule T22. In this study, a W...EGYEL motif in an extended CDR3 $\delta$  loop (85) contacts a disordered region at the end of the  $\alpha$ 2 helix of the T22 molecule from the side (48). The contact residues of the G8 TCR are shown in Fig. 6 (*top middle panel*). Eighty-nine percent of the  $\gamma\delta$  TCR interface with T22 is contributed by the V $\delta$ -chain, with



**FIGURE 6.** Potential contact residues of the V $\gamma$ 2V $\delta$ 2 TCR for a putative Ag presenting molecule-prenyl pyrophosphate complex differs from other unconventional TCRs and conventional TCRs specific for MHC-peptide complexes. The TCRs are oriented with the  $\beta/\gamma$ -chains on the *top left* and the  $\alpha/\delta$ -chains on the *bottom right* of the panels. Contact residues are colored such that those in CDR2 $\alpha/\delta$  are blue, CDR2 $\alpha/\delta$  are magenta, CDR3 $\alpha/\delta$  are yellow, HV4 $\alpha/\delta$  are cyan, CDR1 $\beta/\gamma$  are red, CDR2 $\beta/\gamma$  are orange, and CDR3 $\beta/\gamma$  are green. The diagonal orientation does not attempt to match the docking angle on the MHC/CD1 ligand. *Top panels*, Putative contact residue footprint of the V $\gamma$ 2V $\delta$ 2 TCR based on the effects of point mutations on human V $\gamma$ 2V $\delta$ 2 T cell reactivity to nonpeptide Ag (*top left panel*). Note the potential large contribution of germline-encoded regions of CDR3 $\gamma$  compared with only a minor contribution by L97 in CDR3 $\delta$ . In contrast, the G8  $\gamma\delta$  TCR (*top middle panel*), that is specific for the T22 MHC class Ib molecule, predominantly uses CDR3 $\delta$  for recognition. The iNKT  $\alpha\beta$  TCR (*top right panel*) binding to the CD1d- $\alpha$ -GalCer complex also predominantly uses the CDR3 $\alpha$  region (which corresponds to CDR3 $\delta$ ). *Middle panels*, Conventional  $\alpha\beta$  TCRs specific for MHC class I-foreign peptide complexes generally use both CDR3 $\alpha$  and CDR3 $\beta$  for MHC-peptide recognition in addition to CDR1 and CDR2. *Bottom panels*, Conventional  $\alpha\beta$  TCRs specific for MHC class II-peptide complexes are similar to MHC class I-peptide-specific  $\alpha\beta$  TCRs and involve extensive CDR3 $\alpha$  and CDR3 $\beta$  contacts in addition to CDR1 and CDR2 contacts. Additional examples of  $\alpha\beta$  TCR recognition of MHC-peptide complexes are shown in Supplemental Figs. 4, 5.



67% contributed by the CDR3 $\delta$  loop. Underscoring the importance of the CDR3 $\delta$  loop, swapping of this region for the CDR3 $\alpha$  of an  $\alpha\beta$  TCR is sufficient to confer recognition of T22 (86). All of the  $\gamma\delta$  T cells that recognized T22 have the W...EGYEL sequence motif in CDR3 $\delta$ . Importantly, this motif is commonly derived from the germline-encoded D $\delta$ 2 gene segment and is present on  $\sim$ 0.85% of nonselected murine V $\delta$ 2 chains; this may account for the high frequency of T22-reactive  $\gamma\delta$  T cells (1/50–1/1000) in unimmunized mice (85).

The other example of unconventional innate TCR recognition is human and murine iNKT  $\alpha\beta$  TCR recognition of glycolipids presented by CD1d (49, 87). iNKT TCRs bind CD1d/ $\alpha$ -GalCer in a top-down orientation paralleling the  $\alpha$  helices of CD1d. Again, CDR3 $\alpha$ , which is the equivalent of CDR3 $\delta$ , plays an important role contributing 52% of the buried surface area (BSA) (Fig. 6, *top left panel*). Only the J $\alpha$ 18 region of CDR3 $\alpha$  contacts the CD1d-lipid complex, explaining the use of this J region by the invariant V $\alpha$ 24 chain of the iNKT TCR. Like the G8  $\gamma\delta$  TCR in which CDR3 $\gamma$  contains only two contact residues, CDR3 $\beta$  contains only one contact residue that contributes only 6% of the BSA. Instead, the germline-encoded CDR2 $\beta$  contributes 28% of the BSA. When the contact residues in the iNKT TCR were mutated to alanine, four out of seven CDR3 $\alpha$  loop residues and two out of four

CDR2 $\beta$  abolished recognition, whereas three other residues in other CDRs had no or little effect (88). Thus, despite large differences in the docking orientation of the iNKT  $\alpha\beta$  TCR and the G8  $\gamma\delta$  TCR for their ligands, unconventional recognition by both involves primarily germline-encoded regions in CDR3 $\alpha/\delta$ , with critical contributions from the germline-encoded CDR2 $\beta$  in iNKT TCR.

In contrast to these examples, our study shows a different mode of recognition for the V $\gamma$ 2V $\delta$ 2 TCR that does not rely as heavily on the CDR3 $\alpha/\delta$  region. Instead, CDR3 $\gamma$  appears to be the critical region for prenyl pyrophosphate recognition. Mutation of either Lys108 or Lys109 in the conserved J $\gamma$ 1.2 region abolishes recognition as does altering the CDR3 $\gamma$  length/sequence (29). Moreover, 20–30% of adult V $\gamma$ 2V $\delta$ 2 T cells express an invariant V $\gamma$ 2J $\gamma$ 1.2 sequence, with the rest exhibiting little differences in CDR3 $\gamma$  length while favoring basic residues in the junctional region. Conservation of CDR3 $\gamma$  length may be required to maintain the correct positioning of the J $\gamma$ 1.2 region in the putative prenyl pyrophosphate-binding site (Figs. 4B, 5). We find that the Arg51 $\delta$  and Glu52 $\delta$  residues in CDR2 $\delta$  are also required for recognition and confirm that there is a strong preference for an aliphatic hydrophobic amino acid (generally leucine, isoleucine, or valine, but not proline) at position 97 in CDR3 $\delta$  but find few restrictions

on CDR3 $\delta$  length or sequence. All of these critical residues cluster in or around an area of positive surface potential due to Arg51 $\delta$  and, to a lesser extent, Lys109 $\gamma$ , as determined by *in silico* mutation (Fig. 5).

In addition to this site, we now show that critical residues are also present in exposed areas of CDR1 $\gamma$  and CDR2 $\gamma$  as well as CDR1 $\delta$ . These residues are distant (15.3 Å for Thr29 in CDR1 $\gamma$ , 15.2 Å for Tyr54 in CDR2 $\gamma$ , and 20.1 Å for Glu28 in CDR1 $\delta$ ) from the proposed binding site, making it unlikely that they would directly influence prenyl pyrophosphate binding. Instead, we would propose that these residues contact a presenting molecule for the prenyl pyrophosphates similar to  $\alpha\beta$  TCRs contacting peptide-MHC class I or class II complexes.

The potential footprint of the V $\gamma$ 2V $\delta$ 2 TCR on the putative Ag-presenting molecule shows more similarities than differences with the footprints of conventional  $\alpha\beta$  TCR that bind to MHC class I or class II/foreign peptide complexes (89). Like the V $\gamma$ 2V $\delta$ 2 TCR, most antimicrobial  $\alpha\beta$  TCRs contact their ligands using all six CDRs, although their relative energetic contributions to binding vary (contact residues of TCRs specific for peptide-MHC class I and class II are shown in Fig. 6 and Supplemental Figs. 4, 5). The main exceptions are A6 and B7 TCRs specific for HLA-A2-TAX (57) (Supplemental Fig. 4).

Generally, CDR1 $\alpha$  and CDR2 $\alpha$  are centered over the MHC  $\alpha$ 2 helix, and CDR1 $\beta$  and CDR2 $\beta$  are centered over the MHC  $\alpha$ 1 helix in a diagonal orientation. The CDR3 $\alpha$  region is centered on the N-terminal end of the peptide, and the CDR3 $\beta$  region is centered on the C-terminal end, but both regions can also contact MHC. Centering the diverse CDR3 regions over the peptide allows for the recognition of an array of sequences. Autoimmune recognition of self-peptides represents a major exception to the diagonal orientation of  $\alpha\beta$  TCRs docking to their ligands because autoimmune TCRs may bind with unusual topologies (90) and may shift to docking over the extreme N terminus of the peptide (91). Although the docking orientation of the V $\gamma$ 2V $\delta$ 2 TCR and the structure of the putative presenting molecule is unknown, the similarities between the footprint of antimicrobial  $\alpha\beta$  TCRs and the footprint of the V $\gamma$ 2V $\delta$ 2 TCR would suggest that a presenting molecule is required.

V $\gamma$ 2V $\delta$ 2 TCR recognition also differs from antimicrobial  $\alpha\beta$  TCR recognition in important ways. In contrast to antimicrobial  $\alpha\beta$  TCRs in which most have multiple contact residues in CDR3 $\alpha$  (Fig. 6, Supplemental Figs. 4, 5), the CDR3 $\delta$  region (equivalent to CDR3 $\alpha$ ) makes a limited contribution to recognition because the only preference found was for an aliphatic residue at position 97. Moreover, V $\gamma$ 2V $\delta$ 2 recognition is primarily through the germline-encoded gene segments, CDR1 $\gamma$ , CDR2 $\gamma$ , CDR1 $\delta$ , and CDR2 $\delta$  regions, coupled with V $\gamma$ 2J $\gamma$ 1.2 chains that are either invariant (lacking N nucleotide additions) or with limited diversity in sequence and length.

Given the large footprint for V $\gamma$ 2V $\delta$ 2 TCR, we speculate that there is a presenting molecule for prenyl pyrophosphate Ags. Because there is no evidence for genetic restriction in V $\gamma$ 2V $\delta$ 2 TCR recognition, we would predict that the putative presenting molecule has little or no polymorphisms in contact regions for the TCR. Additionally, because human tumor cells of diverse origin and different hematopoietic APCs present Ag, the putative presenting molecule would need to be widely expressed much like MHC class I molecules. Although prenyl pyrophosphate reactivity is preserved in both New World and Old World monkeys (92, 93), rodent and guinea pig  $\gamma\delta$  T cells (94) are unable to respond to prenyl pyrophosphate Ags nor can rodent, hamster, or other species APCs present prenyl pyrophosphate Ags to human V $\gamma$ 2V $\delta$ 2 T cells (35, 95). There may exist ruminant  $\gamma\delta$  T cells with prenyl

pyrophosphate reactivity, although this has not been definitively established (96). Consistent with the lack of reactivity by most other species, no other nonprimate species has homologous V genes for the V $\gamma$ 2 and V $\delta$ 2 gene segments. Despite the reactivity of monkeys to prenyl pyrophosphates, both Vero and COS-7 cell lines (95) (derived from African green monkeys) are unable to present to human V $\gamma$ 2V $\delta$ 2 T cells. Thus, there may be xenogeneic differences between African green monkeys and humans in the putative presenting molecules. Finally, we would predict that the putative presenting molecule has a structure homologous to MHC class I or class II like all other nonclassical presenting molecules and ligands (CD1, MR1, and MICA/MICB) so far discovered, although none of the known MHC class Ib molecules are viable candidates. It also is possible that the presentation molecule belongs to a new class of presenting molecules, such as an enzyme, a heat shock protein, or an Ig superfamily protein, that is not related in structure to MHC class I/II molecules.

Presentation of prenyl pyrophosphates by a presenting molecule is also supported by functional and TCR binding studies. Recognition of prenyl pyrophosphates requires cell-cell contact for V $\gamma$ 2V $\delta$ 2 T cell activation as assessed by intracellular calcium flux (32) and TNF- $\alpha$  release (33) that is identical to the contact requirement for  $\alpha\beta$  T cell recognition of MHC/peptide complexes but distinct from ligand recognition by hormone and neurotransmitter receptors. Also, there is no evidence for direct recognition of prenyl pyrophosphates because attempts to soak IPP and HMBPP into V $\gamma$ 2V $\delta$ 2 TCR crystals failed (28), and no binding of prenyl pyrophosphates to soluble V $\gamma$ 2V $\delta$ 2 TCRs was noted in equilibrium dialysis or microcalorimetry experiments (C.T. Morita, unpublished observations). Similarly, a monkey V $\gamma$ 2V $\delta$ 2 TCR tetramer does not directly bind HMBPP but will bind to APC when the APCs are incubated with HMBPP or infected with *M. bovis* bacillus Calmette-Guérin (36). This binding was observed with human and monkey but not mouse, rat, or pig cells, demonstrating specificity for primate APCs identical to the results on presentation of prenyl pyrophosphates (33, 97), bisphosphonates (95), alkylamines (97), and photoaffinity prenyl pyrophosphate analogs (35). Binding was abolished by protease treatment of the cell surface, strongly suggesting that the surface binding molecule was a protein (36). Finally, photoaffinity analogs of prenyl pyrophosphates are able to covalently crosslink to protein(s) on the APC surface for presentation, and this binding could be specifically inhibited by an inactive prenyl pyrophosphate analog (35). Taken together, these findings provide additional evidence for the existence of a cell surface-presenting molecule for prenyl pyrophosphate Ags.

As discussed above, recognition of  $\alpha$ -GalCer/CD1d by the iNKT TCR is primarily through germline-encoded invariant V $\alpha$ 24J $\alpha$ 18 CDR3 $\alpha$  and CDR2 $\beta$  regions (49). However, for other lipids, iNKT recognition also requires residues in CDR1 $\alpha$  in addition to the CDR3 $\alpha$  and CDR2 $\beta$  regions. Again, these residues are encoded by germline gene segments (98). Thus, the basic orientation and framework for binding of both human and mouse iNKTs to their respective CD1d molecules and to different lipids is conserved such that others have proposed that the iNKT receptor can be considered to have characteristics of a pattern-recognition receptor (98). However, the fine specificity and binding affinity of iNKT TCR can be affected by the V $\beta$ -chain partner and its CDR3 $\beta$  sequence (87, 99, 100), allowing iNKT TCR to distinguish between a number of different lipids. Similar differences in the CDR3 sequences of the V $\gamma$ 2V $\delta$ 2 TCR also likely affect prenyl pyrophosphate recognition.

Although V $\gamma$ 2V $\delta$ 2 TCRs appear to function like pattern-recognition receptors (101), as proposed for iNKT TCRs (98), this

is not to assert that there is no selection on V $\gamma$ 2V $\delta$ 2 TCRs during development or Ag stimulation, which is a hallmark of adaptive immune recognition. V $\gamma$ 2V $\delta$ 2 TCR selection clearly occurs because V $\gamma$ 2V $\delta$ 2 T cells using the J $\gamma$ 1.2 region and having an aliphatic amino acid at position 97 are preferentially expanded in vitro (31, 102) and overrepresented in adult V $\gamma$ 2V $\delta$ 2 T cells as compared with fetal/thymic V $\gamma$ 2V $\delta$ 2 T cells (79). However, even in fetuses and neonates, there is a very high proportion of V $\gamma$ 2V $\delta$ 2 T cells that respond to prenyl pyrophosphates with two out of two fetal liver and at least three out of eight cord blood V $\gamma$ 2V $\delta$ 2 T cell clones responding (9; data not shown). Also, Davadou et al. (44) found that 22 out of 25 (88%) PHA-derived thymic V $\gamma$ 2V $\delta$ 2 T cells using the V $\gamma$ 2J $\gamma$ 1.2 chain responded to prenyl pyrophosphates and to Daudi. Overall, 30 out of 38 (79%) of thymic V $\gamma$ 2V $\delta$ 2 T cell clones responded (44). In all of these cases, selection by exogenous Ags is unlikely. Therefore, although peripheral selection is likely responsible for the near universal reactivity of V $\gamma$ 2V $\delta$ 2 T cells that is found in adults, a high proportion of V $\gamma$ 2V $\delta$ 2 T cells start out reactive, probably due to constraints in gene rearrangement (103).

Based on our results, we would predict that most of the recognition is mediated by germline-encoded elements of the V $\gamma$ 2V $\delta$ 2 TCR and that there is a presenting molecule for prenyl pyrophosphate Ags. Although only three examples of unconventional recognition have now been molecularly defined, all share the use of certain germline elements of the TCR for recognition, the invariant V $\alpha$ 14J $\alpha$ 24 gene segments for lipid/CD1d recognition (49), a D $\delta$  motif for T10/T22 (48, 85), and, as noted by others (79, 103), the V $\gamma$ 2J $\gamma$ 1.2 chain and the V $\delta$ 2 gene segment for prenyl pyrophosphates. We speculate that unconventional innate  $\gamma\delta$  and  $\alpha\beta$  TCRs containing invariant V chains, highly biased V gene usage, or conserved CDR3 motifs are likely to bind their ligands using the invariant or biased portion of the TCR. Moreover, the portions of invariant chains, biased V genes, or conserved motifs of innate TCRs that contact the ligands seem to favor germline-encoded segments as also suggested by Born and O'Brien (104). Thus, innate TCRs with a single reactivity may have diverse CDR3 regions like V $\gamma$ 2V $\delta$ 2 T cells but would contact their ligands through either germline-encoded CDR1/2 regions in one or both chains or through germline-encoded D and/or J regions in CDR3s. However, unlike T10-specific V $\gamma$ 2V $\delta$ 2 TCR and iNKT TCR, in situations in which both chains are invariant (like the murine dendritic epidermal V $\gamma$ 5V $\delta$ 1 TCR and the murine V $\gamma$ 6V $\delta$ 1 TCR), both CDR3 regions would likely be involved in binding. This type of recognition allows the majority of a given population of  $\gamma\delta$  T cells to react to their Ag either because they express monoclonal TCRs or because the diversity in the CDR3 regions is of less importance.

## Acknowledgments

We thank K. Ness, G. Workalemahu, and C. Jin for critical review of this manuscript.

## Disclosures

The authors have no financial conflicts of interest.

## References

- Gapin, L. 2009. Where do MAIT cells fit in the family of unconventional T cells? *PLoS Biol.* 7: e70.
- Cerundolo, V., J. D. Silk, S. H. Masri, and M. Salio. 2009. Harnessing invariant NKT cells in vaccination strategies. *Nat. Rev. Immunol.* 9: 28–38.
- Kronenberg, M., and I. Engel. 2007. On the road: progress in finding the unique pathway of invariant NKT cell differentiation. *Curr. Opin. Immunol.* 19: 186–193.
- Morita, C. T., C. M. Parker, M. B. Brenner, and H. Band. 1994. TCR usage and functional capabilities of human  $\gamma\delta$  T cells at birth. *J. Immunol.* 153: 3979–3988.

- Parker, C. M., V. Groh, H. Band, S. A. Porcelli, C. Morita, M. Fabbri, D. Glass, J. L. Strominger, and M. B. Brenner. 1990. Evidence for extrathymic changes in the T cell receptor  $\gamma\delta$  repertoire. *J. Exp. Med.* 171: 1597–1612.
- Morita, C. T., C. Jin, G. Sarikonda, and H. Wang. 2007. Nonpeptide antigens, presentation mechanisms, and immunological memory of human V $\gamma$ 2V $\delta$ 2 T cells: discriminating friend from foe through the recognition of prenyl pyrophosphate antigens. *Immunol. Rev.* 215: 59–76.
- Tanaka, Y., C. T. Morita, Y. Tanaka, E. Nieves, M. B. Brenner, and B. R. Bloom. 1995. Natural and synthetic non-peptide antigens recognized by human  $\gamma\delta$  T cells. *Nature* 375: 155–158.
- Hintz, M., A. Reichenberg, B. Altincicek, U. Bahr, R. M. Gschwind, A.-K. Kollas, E. Beck, J. Wiesner, M. Eberl, and H. Jomaa. 2001. Identification of (*E*)-4-hydroxy-3-methyl-but-2-enyl pyrophosphate as a major activator for human  $\gamma\delta$  T cells in *Escherichia coli*. *FEBS Lett.* 509: 317–322.
- Puan, K.-J., C. Jin, H. Wang, G. Sarikonda, A. M. Raker, H. K. Lee, M. I. Samuelson, E. Märker-Hermann, L. Pasa-Tolic, E. Nieves, et al. 2007. Preferential recognition of a microbial metabolite by human V $\gamma$ 2V $\delta$ 2 T cells. *Int. Immunol.* 19: 657–673.
- Kunzmann, V., E. Bauer, and M. Wilhelm. 1999.  $\gamma\delta$  T-cell stimulation by pamidronate. *N. Engl. J. Med.* 340: 737–738.
- Sanders, J. M., S. Ghosh, J. M. W. Chan, G. Meints, H. Wang, A. M. Raker, Y. Song, A. Colantino, A. Burzynska, P. Kafarski, et al. 2004. Quantitative structure-activity relationships for  $\gamma\delta$  T cell activation by bisphosphonates. *J. Med. Chem.* 47: 375–384.
- Bukowski, J. F., C. T. Morita, and M. B. Brenner. 1999. Human  $\gamma\delta$  T cells recognize alkylamines derived from microbes, edible plants, and tea: implications for innate immunity. *Immunity* 11: 57–65.
- Gober, H. J., M. Kistowska, L. Angman, P. Jenö, L. Mori, and G. De Libero. 2003. Human T cell receptor  $\gamma\delta$  cells recognize endogenous mevalonate metabolites in tumor cells. *J. Exp. Med.* 197: 163–168.
- Thompson, K., J. Rojas-Navea, and M. J. Rogers. 2006. Alkylamines cause V $\gamma$ 9V $\delta$ 2 T-cell activation and proliferation by inhibiting the mevalonate pathway. *Blood* 107: 651–654.
- De Rosa, S. C., J. P. Andrus, S. P. Perfetto, J. J. Mantovani, L. A. Herzenberg, L. A. Herzenberg, and M. Roederer. 2004. Ontogeny of  $\gamma\delta$  T cells in humans. *J. Immunol.* 172: 1637–1645.
- Shen, Y., D. Zhou, L. Qiu, X. Lai, M. Simon, L. Shen, Z. Kou, Q. Wang, L. Jiang, J. Estep, et al. 2002. Adaptive immune response of V $\gamma$ 2V $\delta$ 2<sup>+</sup> T cells during mycobacterial infections. *Science* 295: 2255–2258.
- García, V. E., P. A. Sieling, J.-H. Gong, P. F. Barnes, K. Uyemura, Y. Tanaka, B. R. Bloom, C. T. Morita, and R. L. Modlin. 1997. Single-cell cytokine analysis of  $\gamma\delta$  T cell responses to nonpeptide mycobacterial antigens. *J. Immunol.* 159: 1328–1335.
- Morita, C. T., S. Verma, P. Aparicio, C. Martinez, H. Spits, and M. B. Brenner. 1991. Functionally distinct subsets of human  $\gamma\delta$  T cells. *Eur. J. Immunol.* 21: 2999–3007.
- Cipriani, B., G. Borsellino, F. Poccia, R. Placido, D. Tramonti, S. Bach, L. Battistini, and C. F. Brosnan. 2000. Activation of C-C  $\beta$ -chemokines in human peripheral blood  $\gamma\delta$  T cells by isopentenyl pyrophosphate and regulation by cytokines. *Blood* 95: 39–47.
- Tikhonov, I., C. O. Deetz, R. Paca, S. Berg, V. Lukyanenko, J. K. Lim, and C. D. Pauza. 2006. Human V $\gamma$ 2V $\delta$ 2 T cells contain cytoplasmic RANTES. *Int. Immunol.* 18: 1243–1251.
- Spada, F. M., E. P. Grant, P. J. Peters, M. Sugita, A. Melián, D. S. Leslie, H. K. Lee, E. van Donselaar, D. A. Hanson, A. M. Krensky, et al. 2000. Self-recognition of CD1 by  $\gamma\delta$  T cells: implications for innate immunity. *J. Exp. Med.* 191: 937–948.
- Dieli, F., M. Troye-Blomberg, J. Ivanyi, J. J. Fournié, A. M. Krensky, M. Bonneville, M. A. Peyrat, N. Caccamo, G. Sireci, and A. Salerno. 2001. Granulysin-dependent killing of intracellular and extracellular *Mycobacterium tuberculosis* by V $\gamma$ 9/V $\delta$ 2 T lymphocytes. *J. Infect. Dis.* 184: 1082–1085.
- Dudal, S., C. Turriere, S. Bessoles, P. Fontes, F. Sanchez, J. Liautard, J. P. Liautard, and V. Lafont. 2006. Release of LL-37 by activated human V $\gamma$ 9V $\delta$ 2 T cells: a microbicidal weapon against *Brucella suis*. *J. Immunol.* 177: 5533–5539.
- Wilhelm, M., V. Kunzmann, S. Eckstein, P. Reimer, F. Weissinger, T. Ruediger, and H.-P. Tony. 2003.  $\gamma\delta$  T cells for immune therapy of patients with lymphoid malignancies. *Blood* 102: 200–206.
- Dieli, F., D. Vermijlen, F. Fulfaro, N. Caccamo, S. Meraviglia, G. Cicero, A. Roberts, S. Buccheri, M. D'Asaro, N. Gebbia, et al. 2007. Targeting human  $\gamma\delta$  T cells with zoledronate and interleukin-2 for immunotherapy of hormone-refractory prostate cancer. *Cancer Res.* 67: 7450–7457.
- Bukowski, J. F., C. T. Morita, Y. Tanaka, B. R. Bloom, M. B. Brenner, and H. Band. 1995. V $\gamma$ 2V $\delta$ 2 TCR-dependent recognition of non-peptide antigens and Daudi cells analyzed by TCR gene transfer. *J. Immunol.* 154: 998–1006.
- Morita, C. T., H. K. Lee, H. Wang, H. Li, R. A. Mariuzza, and Y. Tanaka. 2001. Structural features of nonpeptide prenyl pyrophosphates that determine their antigenicity for human  $\gamma\delta$  T cells. *J. Immunol.* 167: 36–41.
- Allison, T. J., C. C. Winter, J. J. Fournié, M. Bonneville, and D. N. Garboczi. 2001. Structure of a human  $\gamma\delta$  T-cell antigen receptor. *Nature* 411: 820–824.
- Bukowski, J. F., C. T. Morita, H. Band, and M. B. Brenner. 1998. Crucial role of TCR $\gamma$  chain junctional region in prenyl pyrophosphate antigen recognition by  $\gamma\delta$  T cells. *J. Immunol.* 161: 286–293.
- Miyagawa, F., Y. Tanaka, S. Yamashita, B. Mikami, K. Danno, M. Uehara, and N. Minato. 2001. Essential contribution of germline-encoded lysine residues in J $\gamma$ 1.2 segment to the recognition of nonpeptide antigens by human  $\gamma\delta$  T cells. *J. Immunol.* 167: 6773–6779.

31. Yamashita, S., Y. Tanaka, M. Harazaki, B. Mikami, and N. Minato. 2003. Recognition mechanism of non-peptide antigens by human  $\gamma\delta$  T cells. *Int. Immunol.* 15: 1301–1307.
32. Morita, C. T., E. M. Beckman, J. F. Bukowski, Y. Tanaka, H. Band, B. R. Bloom, D. E. Golan, and M. B. Brenner. 1995. Direct presentation of nonpeptide prenyl pyrophosphate antigens to human  $\gamma\delta$  T cells. *Immunity* 3: 495–507.
33. Lang, F., M. A. Peyrat, P. Constant, F. Davodeau, J. David-Ameline, Y. Poquet, H. Vié, J. J. Fourmié, and M. Bonneville. 1995. Early activation of human V $\gamma$ 9V $\delta$ 2 T cell broad cytotoxicity and TNF production by nonpeptidic mycobacterial ligands. *J. Immunol.* 154: 5986–5994.
34. Pichler, W. J., A. Beeler, M. Keller, M. Lerch, S. Posadas, D. Schmid, Z. Spanou, A. Zawodniak, and B. Gerber. 2006. Pharmacological interaction of drugs with immune receptors: the p-i concept. *Allergol. Int.* 55: 17–25.
35. Sarikonda, G., H. Wang, K.-J. Puan, X.-H. Liu, H. K. Lee, Y. Song, M. D. Distefano, E. Oldfield, G. D. Prestwich, and C. T. Morita. 2008. Photo-affinity antigens for human  $\gamma\delta$  T cells. *J. Immunol.* 181: 7738–7750.
36. Wei, H., D. Huang, X. Lai, M. Chen, W. Zhong, R. Wang, and Z. W. Chen. 2008. Definition of APC presentation of phosphoantigen (*E*)-4-hydroxy-3-methyl-but-2-enyl pyrophosphate to V $\gamma$ 2V $\delta$ 2 TCR. *J. Immunol.* 181: 4798–4806.
37. Saito, T., A. Weiss, J. Miller, M. A. Norcross, and R. N. Germain. 1987. Specific antigen-Ia activation of transfected human T cells expressing murine T $\beta$   $\alpha$ -human T3 receptor complexes. *Nature* 325: 125–130.
38. Wang, H., H. K. Lee, J. F. Bukowski, H. Li, R. A. Mariuzza, Z. W. Chen, K.-H. Nam, and C. T. Morita. 2003. Conservation of nonpeptide antigen recognition by rhesus monkey V $\gamma$ 2V $\delta$ 2 T cells. *J. Immunol.* 170: 3696–3706.
39. Giner, J.-L. 2002. A convenient synthesis of (*E*)-4-hydroxy-3-methyl-2-butenyl pyrophosphate and its [<sup>14</sup>C]-labeled form. *Tetrahedron Lett.* 43: 5457–5459.
40. Puan, K.-J., H. Wang, T. Dairi, T. Kuzuyama, and C. T. Morita. 2005. *fldA* is an essential gene required in the 2-*C*-methyl-D-erythritol 4-phosphate pathway for isoprenoid biosynthesis. *FEBS Lett.* 579: 3802–3806.
41. Grant, E. P., M. Degano, J. P. Rosat, S. Stenger, R. L. Modlin, I. A. Wilson, S. A. Porcellii, and M. B. Brenner. 1999. Molecular recognition of lipid antigens by T cell receptors. *J. Exp. Med.* 189: 195–205.
42. Morita, C. T., H. Li, J. G. Lamphear, R. R. Rich, J. D. Fraser, R. A. Mariuzza, and H. K. Lee. 2001. Superantigen recognition by  $\gamma\delta$  T cells: SEA recognition site for human V $\gamma$ 2 T cell receptors. *Immunity* 14: 331–344.
43. Tanaka, Y., S. Sano, E. Nieves, G. De Libero, D. Rosa, R. L. Modlin, M. B. Brenner, B. R. Bloom, and C. T. Morita. 1994. Nonpeptide ligands for human  $\gamma\delta$  T cells. *Proc. Natl. Acad. Sci. USA* 91: 8175–8179.
44. Davodeau, F., M.-A. Peyrat, M.-M. Hallet, J. Gaschet, I. Houde, R. Vivien, H. Vie, and M. Bonneville. 1993. Close correlation between Daudi and mycobacterial antigen recognition by human  $\gamma\delta$  T cells and expression of V9JPC1  $\gamma$ /V2DJC8-encoded T cell receptors. *J. Immunol.* 151: 1214–1223.
45. De Libero, G., G. Casorati, C. Giachino, C. Carbonara, N. Migone, P. Matzinger, and A. Lanzavecchia. 1991. Selection by two powerful antigens may account for the presence of the major population of human peripheral  $\gamma\delta$  T cells. *J. Exp. Med.* 173: 1311–1322.
46. Bender, A., B. Heckl-Ostreicher, E. J. M. Grondal, and D. Kabelitz. 1993. Clonal specificity of human  $\gamma\delta$  T cells: V $\gamma$ 9\* T-cell clones frequently recognize *Plasmodium falciparum* merozoites, *Mycobacterium tuberculosis*, and group-A streptococci. *Int. Arch. Allergy Immunol.* 100: 12–18.
47. Baker, N. A., D. Sept, S. Joseph, M. J. Holst, and J. A. McCammon. 2001. Electrostatics of nanosystems: application to microtubules and the ribosome. *Proc. Natl. Acad. Sci. USA* 98: 10037–10041.
48. Adams, E. J., Y. H. Chien, and K. C. Garcia. 2005. Structure of a  $\gamma\delta$  T cell receptor in complex with the nonclassical MHC T22. *Science* 308: 227–231.
49. Borg, N. A., K. S. Wun, L. Kjer-Nielsen, M. C. Wilce, D. G. Pellicci, R. Koh, G. S. Besra, M. Bharadwaj, D. I. Godfrey, J. McCluskey, and J. Rossjohn. 2007. CD1d-lipid-antigen recognition by the semi-invariant NKT T-cell receptor. *Nature* 448: 44–49.
50. Tynan, F. E., H. H. Reid, L. Kjer-Nielsen, J. J. Miles, M. C. Wilce, M. Kostenko, N. A. Borg, N. A. Williamson, T. Beddoe, A. W. Purcell, et al. 2007. A T cell receptor flattens a bulged antigenic peptide presented by a major histocompatibility complex class I molecule. *Nat. Immunol.* 8: 268–276.
51. Gagnon, S. J., O. Y. Borbulevich, R. L. Davis-Harrison, R. V. Turner, M. Damirjian, A. Wojnarowicz, W. E. Biddison, and B. M. Baker. 2006. T cell receptor recognition via cooperative conformational plasticity. *J. Mol. Biol.* 363: 228–243.
52. Garboczi, D. N., P. Ghosh, U. Utz, Q. R. Fan, W. E. Biddison, and D. C. Wiley. 1996. Structure of the complex between human T-cell receptor, viral peptide and HLA-A2. *Nature* 384: 134–141.
53. Kjer-Nielsen, L., C. S. Clements, A. W. Purcell, A. G. Brooks, J. C. Whisstock, S. R. Burrows, J. McCluskey, and J. Rossjohn. 2003. A structural basis for the selection of dominant  $\alpha\beta$  T cell receptors in antiviral immunity. *Immunity* 18: 53–64.
54. Garcia, K. C., M. Degano, L. R. Pease, M. Huang, P. A. Peterson, L. Teyton, and I. A. Wilson. 1998. Structural basis of plasticity in T cell receptor recognition of a self peptide-MHC antigen. *Science* 279: 1166–1172.
55. Colf, L. A., A. J. Bankovich, N. A. Hanick, N. A. Bowerman, L. L. Jones, D. M. Kranz, and K. C. Garcia. 2007. How a single T cell receptor recognizes both self and foreign MHC. *Cell* 129: 135–146.
56. Buslepp, J., H. Wang, W. E. Biddison, E. Appella, and E. J. Collins. 2003. A correlation between TCR V $\alpha$  docking on MHC and CD8 dependence: implications for T cell selection. *Immunity* 19: 595–606.
57. Ding, Y. H., K. J. Smith, D. N. Garboczi, U. Utz, W. E. Biddison, and D. C. Wiley. 1998. Two human T cell receptors bind in a similar diagonal mode to the HLA-A2/Tax peptide complex using different TCR amino acids. *Immunity* 8: 403–411.
58. Stewart-Jones, G. B., A. J. McMichael, J. I. Bell, D. I. Stuart, and E. Y. Jones. 2003. A structural basis for immunodominant human T cell receptor recognition. *Nat. Immunol.* 4: 657–663.
59. Reiser, J. B., C. Grégoire, C. Darnault, T. Mosser, A. Guimezanes, A. M. Schmitt-Verhulst, J. C. Fontecilla-Camps, G. Mazza, B. Malissen, and D. Housset. 2002. A T cell receptor CDR3 $\beta$  loop undergoes conformational changes of unprecedented magnitude upon binding to a peptide/MHC class I complex. *Immunity* 16: 345–354.
60. Hoare, H. L., L. C. Sullivan, G. Pietra, C. S. Clements, E. J. Lee, L. K. Ely, T. Beddoe, M. Falco, L. Kjer-Nielsen, H. H. Reid, et al. 2006. Structural basis for a major histocompatibility complex class Ib-restricted T cell response. *Nat. Immunol.* 7: 256–264.
61. Tynan, F. E., S. R. Burrows, A. M. Buckle, C. S. Clements, N. A. Borg, J. J. Miles, T. Beddoe, J. C. Whisstock, M. C. Wilce, S. L. Silins, et al. 2005. T cell receptor recognition of a 'super-bulged' major histocompatibility complex class I-bound peptide. *Nat. Immunol.* 6: 1114–1122.
62. Reiser, J. B., C. Darnault, C. Grégoire, T. Mosser, G. Mazza, A. Kearney, P. A. van der Merwe, J. C. Fontecilla-Camps, D. Housset, and B. Malissen. 2003. CDR3 loop flexibility contributes to the degeneracy of TCR recognition. *Nat. Immunol.* 4: 241–247.
63. Reiser, J. B., C. Darnault, A. Guimezanes, C. Grégoire, T. Mosser, A. M. Schmitt-Verhulst, J. C. Fontecilla-Camps, B. Malissen, D. Housset, and G. Mazza. 2000. Crystal structure of a T cell receptor bound to an allogeneic MHC molecule. *Nat. Immunol.* 1: 291–297.
64. Mazza, C., N. Auphan-Anezin, C. Grégoire, A. Guimezanes, C. Kellenberger, A. Roussel, A. Kearney, P. A. van der Merwe, A. M. Schmitt-Verhulst, and B. Malissen. 2007. How much can a T-cell antigen receptor adapt to structurally distinct antigenic peptides? *EMBO J.* 26: 1972–1983.
65. Gras, S., S. R. Burrows, L. Kjer-Nielsen, C. S. Clements, Y. C. Liu, L. C. Sullivan, M. J. Bell, A. G. Brooks, A. W. Purcell, J. McCluskey, and J. Rossjohn. 2009. The shaping of T cell receptor recognition by self-tolerance. *Immunity* 30: 193–203.
66. Reinherz, E. L., K. Tan, L. Tang, P. Kern, J. Liu, Y. Xiong, R. E. Hussey, A. Smolyar, B. Hare, R. Zhang, et al. 1999. The crystal structure of a T cell receptor in complex with peptide and MHC class II. *Science* 286: 1913–1921.
67. Hennecke, J., A. Carfi, and D. C. Wiley. 2000. Structure of a covalently stabilized complex of a human  $\alpha\beta$  T-cell receptor, influenza HA peptide and MHC class II molecule, HLA-DR1. *EMBO J.* 19: 5611–5624.
68. Maynard, J., K. Petersson, D. H. Wilson, E. J. Adams, S. E. Blondelle, M. J. Boulanger, D. B. Wilson, and K. C. Garcia. 2005. Structure of an auto-immune T cell receptor complexed with class II peptide-MHC: insights into MHC bias and antigen specificity. *Immunity* 22: 81–92.
69. Li, Y., Y. Huang, J. Lue, J. A. Quandt, R. Martin, and R. A. Mariuzza. 2005. Structure of a human autoimmunity TCR bound to a myelin basic protein self-peptide and a multiple sclerosis-associated MHC class II molecule. *EMBO J.* 24: 2968–2979.
70. Deng, L., R. J. Langley, P. H. Brown, G. Xu, L. Teng, Q. Wang, M. I. Gonzales, G. G. Callender, M. I. Nishimura, S. L. Topalian, and R. A. Mariuzza. 2007. Structural basis for the recognition of mutant self by a tumor-specific, MHC class II-restricted T cell receptor. *Nat. Immunol.* 8: 398–408.
71. Dai, S., E. S. Huseby, K. Rubtsova, J. Scott-Browne, F. Crawford, W. A. Macdonald, P. Marrack, and J. W. Kappler. 2008. Crossreactive T cells spotlight the germline rules for  $\alpha\beta$  T cell-receptor interactions with MHC molecules. *Immunity* 28: 324–334.
72. Brenner, M. B., J. L. Strominger, and M. S. Krangel. 1988. The  $\gamma\delta$  T cell receptor. *Adv. Immunol.* 43: 133–192.
73. Heilig, J. S., and S. Tonegawa. 1986. Diversity of murine  $\gamma$  genes and expression in fetal and adult T lymphocytes. *Nature* 322: 836–840.
74. Scotet, E., L. O. Martinez, E. Grant, R. Barbaras, P. Jenö, M. Guiraud, B. Monsarrat, X. Saulquin, S. Maillat, J. P. Estève, et al. 2005. Tumor recognition following V $\gamma$ 9V $\delta$ 2 T cell receptor interactions with a surface F1-AT-Pase-related structure and apolipoprotein A-I. *Immunity* 22: 71–80.
75. Delfau, M.-H., A. J. Hance, D. Lecossier, E. Vilmer, and B. Grandchamp. 1992. Restricted diversity of V $\gamma$ 9-JP rearrangements in unstimulated human  $\gamma\delta$  T lymphocytes. *Eur. J. Immunol.* 22: 2437–2443.
76. Davis, M. M., and P. J. Bjorkman. 1988. T-cell antigen receptor genes and T-cell recognition. *Nature* 334: 395–402.
77. Rock, E. P., P. R. Sibal, M. M. Davis, and Y. H. Chien. 1994. CDR3 length in antigen-specific immune receptors. *J. Exp. Med.* 179: 323–328.
78. Allison, T. J., and D. N. Garboczi. 2002. Structure of  $\gamma\delta$  T cell receptors and their recognition of non-peptide antigens. *Mol. Immunol.* 38: 1051–1061.
79. Davodeau, F., M. A. Peyrat, M. M. Hallet, I. Houde, H. Vie, and M. Bonneville. 1993. Peripheral selection of antigen receptor junctional features in a major human  $\gamma\delta$  subset. *Eur. J. Immunol.* 23: 804–808.
80. Borg, N. A., L. K. Ely, T. Beddoe, W. A. Macdonald, H. H. Reid, C. S. Clements, A. W. Purcell, L. Kjer-Nielsen, J. J. Miles, S. R. Burrows, et al. 2005. The CDR3 regions of an immunodominant T cell receptor dictate the 'energetic landscape' of peptide-MHC recognition. *Nat. Immunol.* 6: 171–180.
81. Manning, T. C., C. J. Schlueter, T. C. Brodnicki, E. A. Parke, J. A. Speir, K. C. Garcia, L. Teyton, I. A. Wilson, and D. M. Kranz. 1998. Alanine scanning mutagenesis of an  $\alpha\beta$  T cell receptor: mapping the energy of antigen recognition. *Immunity* 8: 413–425.

82. Ishizuka, J., G. B. E. Stewart-Jones, A. van der Merwe, J. I. Bell, A. J. McMichael, and E. Y. Jones. 2008. The structural dynamics and energetics of an immunodominant T cell receptor are programmed by its V $\beta$  domain. *Immunity* 28: 171–182.
83. Havran, W. L., Y. H. Chien, and J. P. Allison. 1991. Recognition of self antigens by skin-derived T cells with invariant  $\gamma\delta$  antigen receptors. *Science* 252: 1430–1432.
84. Porcelli, S., C. E. Yockey, M. B. Brenner, and S. P. Balk. 1993. Analysis of T cell antigen receptor (TCR) expression by human peripheral blood CD4<sup>8</sup>  $\alpha\beta$  T cells demonstrates preferential use of several V $\beta$  genes and an invariant TCR  $\alpha$  chain. *J. Exp. Med.* 178: 1–16.
85. Shin, S., R. El-Diwany, S. Schaffert, E. J. Adams, K. C. Garcia, P. Pereira, and Y.-H. Chien. 2005. Antigen recognition determinants of  $\gamma\delta$  T cell receptors. *Science* 308: 252–255.
86. Adams, E. J., P. Strop, S. Shin, Y. H. Chien, and K. C. Garcia. 2008. An autonomous CDR3 $\delta$  is sufficient for recognition of the nonclassical MHC class I molecules T10 and T22 by  $\gamma\delta$  T cells. *Nat. Immunol.* 9: 777–784.
87. Pellicci, D. G., O. Patel, L. Kjer-Nielsen, S. S. Pang, L. C. Sullivan, K. Kyparissoudis, A. G. Brooks, H. H. Reid, S. Gras, I. S. Lucet, et al. 2009. Differential recognition of CD1d- $\alpha$ -galactosyl ceramide by the V $\beta$ 8.2 and V $\beta$  7 semi-invariant NKT T cell receptors. *Immunity* 31: 47–59.
88. Wun, K. S., N. A. Borg, L. Kjer-Nielsen, T. Beddoe, R. Koh, S. K. Richardson, M. Thakur, A. R. Howell, J. P. Scott-Browne, L. Gapin, et al. 2008. A minimal binding footprint on CD1d-glycolipid is a basis for selection of the unique human NKT TCR. *J. Exp. Med.* 205: 939–949.
89. Godfrey, D. I., J. Rossjohn, and J. McCluskey. 2008. The fidelity, occasional promiscuity, and versatility of T cell receptor recognition. *Immunity* 28: 304–314.
90. Hahn, M., M. J. Nicholson, J. Pyrdol, and K. W. Wucherpfennig. 2005. Unconventional topology of self peptide-major histocompatibility complex binding by a human autoimmune T cell receptor. *Nat. Immunol.* 6: 490–496.
91. Deng, L., and R. A. Mariuzza. 2007. Recognition of self-peptide-MHC complexes by autoimmune T-cell receptors. *Trends Biochem. Sci.* 32: 500–508.
92. Sicard, H., S. Ingoure, B. Luciani, C. Serraz, J.-J. Fourmié, M. Bonneville, J. Tiollier, and F. Romagné. 2005. *In vivo* immunomanipulation of V $\gamma$ 9V $\delta$ 2 T cells with a synthetic phosphoantigen in a preclinical nonhuman primate model. *J. Immunol.* 175: 5471–5480.
93. Daubenberger, C. A., M. Salomon, W. Vecino, B. Hübner, H. Troll, R. Rodrigues, M. E. Patarroyo, and G. Pluschke. 2001. Functional and structural similarity of V $\gamma$ 9V $\delta$ 2 T cells in humans and *Aotus* monkeys, a primate infection model for *Plasmodium falciparum* malaria. *J. Immunol.* 167: 6421–6430.
94. Xiong, X., C. T. Morita, J. F. Bukowski, M. B. Brenner, and C. C. Dascher. 2004. Identification of guinea pig  $\gamma\delta$  T cells and characterization during pulmonary tuberculosis. *Vet. Immunol. Immunopathol.* 102: 33–44.
95. Kato, Y., Y. Tanaka, H. Tanaka, S. Yamashita, and N. Minato. 2003. Requirement of species-specific interactions for the activation of human  $\gamma\delta$  T cells by pamidronate. *J. Immunol.* 170: 3608–3613.
96. Welsh, M. D., H. E. Kennedy, A. J. Smyth, R. M. Girvin, P. Andersen, and J. M. Pollock. 2002. Responses of bovine WC1<sup>+</sup>  $\gamma\delta$  T cells to protein and nonprotein antigens of *Mycobacterium bovis*. *Infect. Immun.* 70: 6114–6120.
97. Green, A. E., A. Lissina, S. L. Hutchinson, R. E. Hewitt, B. Temple, D. James, J. M. Boulter, D. A. Price, and A. K. Sewell. 2004. Recognition of nonpeptide antigens by human V $\gamma$ 9V $\delta$ 2 T cells requires contact with cells of human origin. *Clin. Exp. Immunol.* 136: 472–482.
98. Scott-Browne, J. P., J. L. Matsuda, T. Mallevaey, J. White, N. A. Borg, J. McCluskey, J. Rossjohn, J. Kappler, P. Marrack, and L. Gapin. 2007. Germline-encoded recognition of diverse glycolipids by natural killer T cells. *Nat. Immunol.* 8: 1105–1113.
99. Mallevaey, T., J. P. Scott-Browne, J. L. Matsuda, M. H. Young, D. G. Pellicci, O. Patel, M. Thakur, L. Kjer-Nielsen, S. K. Richardson, V. Cerundolo, et al. 2009. T cell receptor CDR2 $\beta$  and CDR3 $\beta$  loops collaborate functionally to shape the iNKT cell repertoire. *Immunity* 31: 60–71.
100. Florence, W. C., C. Xia, L. E. Gordy, W. Chen, Y. Zhang, J. Scott-Browne, Y. Kinjo, K. O. Yu, S. Keshipeddy, D. G. Pellicci, et al. 2009. Adaptability of the semi-invariant natural killer T-cell receptor towards structurally diverse CD1d-restricted ligands. *EMBO J.* 28: 3579–3590.
101. Morita, C. T., R. A. Mariuzza, and M. B. Brenner. 2000. Antigen recognition by human  $\gamma\delta$  T cells: pattern recognition by the adaptive immune system. *Springer Semin. Immunopathol.* 22: 191–217.
102. Evans, P. S., P. J. Enders, C. Yin, T. J. Ruckwardt, M. Malkovsky, and C. D. Pauza. 2001. *In vitro* stimulation with a non-peptidic alkylphosphate expands cells expressing V $\gamma$ 2-J $\gamma$ 1.2/V $\delta$ 2 T-cell receptors. *Immunology* 104: 19–27.
103. Chien, Y.-H., and M. Bonneville. 2006.  $\gamma\delta$  T cell receptors. *Cell. Mol. Life Sci.* 63: 2089–2094.
104. Born, W. K., and R. L. O'Brien. 2009. Antigen-restricted  $\gamma\delta$  T-cell receptors? *Arch. Immunol. Ther. Exp. (Warsz.)* 57: 129–135.